




Article

Determination and Similarity Analysis of PM_{2.5} Emission Source Profiles Based on Organic Markers for Monterrey, Mexico

Yasmany Mancilla ¹, Gerardo Medina ¹, Lucy T. González ¹, Pierre Herckes ², Matthew P. Fraser ³
and Alberto Mendoza ^{1,*}

¹ School of Engineering and Sciences, Tecnológico de Monterrey, Ave. Eugenio Garza Sada 2501, Monterrey 64849, Mexico; y.mancilla@tec.mx (Y.M.); gerardo.medina89@gmail.com (G.M.); lucy.gonzalez@tec.mx (L.T.G.)

² School of Molecular Sciences, Arizona State University, Tempe, AZ 85287, USA; Pierre.Herckes@asu.edu

³ School of Sustainable Engineering and the Built Environment, Arizona State University, Tempe, AZ 85287, USA; matthew.fraser@asu.edu

* Correspondence: mendoza.alberto@tec.mx

Abstract: Source attribution of airborne particulate matter (PM) relies on a host of different chemical species. Organic molecular markers are a set of particularly useful marker compounds for estimating source contributions to the fine PM fraction (i.e., PM_{2.5}). Although there are many source apportionment studies based on organic markers, these studies heavily rely on the few studies that report region-specific emission profiles. Source attribution efforts, particularly those conducted in countries with emerging economies, benefit from ad hoc information to conduct the corresponding analyses. In this study, we report organic molecular marker source profiles for PM_{2.5} emitted from 12 major sources types from five general source categories (meat cooking operations, vehicle exhausts, industries, biomass and trash burning, and urban background) for the Monterrey Metropolitan Area (Mexico). Source emission samples were obtained from a ground-based source-dominated sampling approach. Filter-based instruments were utilized, and the loaded filters were chemically characterized for organic markers by GC-MS. Levoglucosan and cholesterol dominate charbroiled-cooking operation sources while methoxyphenols, PAHs and hopanes dominate open-waste burning, vehicle exhaust and industrial emissions, respectively. A statistical analysis showed values of the Pearson distance < 0.4 and the similarity identity distance > 0.8 in all cases, indicating dissimilar source profiles. This was supported by the coefficient of divergence average values that ranged from 0.62 to 0.72. These profiles could further be utilized in receptor models to conduct source apportionment in regions with similar characteristics and can also be used to develop air pollution abatement strategies.

Keywords: fine particulate matter; organic aerosol; diagnostic ratios; source attribution



Citation: Mancilla, Y.; Medina, G.; González, L.T.; Herckes, P.; Fraser, M.P.; Mendoza, A. Determination and Similarity Analysis of PM_{2.5} Emission Source Profiles Based on Organic Markers for Monterrey, Mexico. *Atmosphere* **2021**, *12*, 554. <https://doi.org/10.3390/atmos12050554>

Academic Editors: Markus Furger and Gaëlle Uzu

Received: 5 March 2021

Accepted: 16 April 2021

Published: 26 April 2021

Publisher's Note: MDPI stays neutral with regard to jurisdictional claims in published maps and institutional affiliations.



Copyright: © 2021 by the authors. Licensee MDPI, Basel, Switzerland. This article is an open access article distributed under the terms and conditions of the Creative Commons Attribution (CC BY) license (<https://creativecommons.org/licenses/by/4.0/>).

1. Introduction

Fine organic carbon (OC) aerosol plays a major role in environmental impacts and health risks derived from air pollution exposure [1–3]. As part of the urban air pollution by PM_{2.5} (fine particles with aerodynamic diameters less than 2.5 μm), the levels of OC have become a central issue in decision making in improving air quality in urban areas [4,5]. Fine OC is frequently the major fraction of the ambient PM_{2.5} mass in urban environments [6,7]. Fine OC is a complex mixture of hundreds of organic compounds that are directly emitted or generated by atmospheric chemical processes [8–10]. Despite these organic compounds being toxic and carcinogenic [11], some can be useful as markers to perform source attribution studies at specific sites. These chemical markers are present in relatively high concentrations in emissions from specific sources and in low concentrations in other sources, and they react slowly enough in the atmosphere such that their origins can be tracked during their transport from the sources to the receptor sites [12–14]. Organic

markers that have been used in the past include organic compounds from the families of sugars, steroids, methoxyphenols, resin acids, *n*-alkanes, *n*-alkanoic acids, hopanes (pentacyclic triterpenes), and polycyclic aromatic hydrocarbons (PAHs) [15].

Much research related to source apportionment studies has focused on using trace elements, particularly metals, as chemical markers (e.g., [16]); however, most metals can be emitted from multiple types of sources, and thus source apportionment using only elemental data has become difficult [14]. The use of organic compounds in source apportionment studies has the advantage that some of them are exclusively characteristic of specific chemical source fingerprints and can be used in the source attribution process [14]. Thus, the use of organic markers has been helpful in distinguishing types of source emissions in source apportionment studies around the world (e.g., [17]). In particular, the use of organic markers to construct source profiles and their application to source attribution using a chemical mass balance approach has proven fruitful [4].

Despite the proven usefulness of source profiles constructed from organic markers, few studies have developed these for emission sources specific to regions that experience severe air pollution episodes in countries with emerging economies [17,18]. Although several source apportionment approaches do not explicitly require chemical source fingerprints to perform the analysis (e.g., using positive matrix factorization, PMF), they do benefit from a benchmark to support the interpretation of the results. If a chemical mass balance approach is followed, source profiles are a fundamental part of the attribution process. A normal practice has been to assume that a set of source profiles derived for a given region or regions can be used in a source attribution study for another set; however, it has been recognized that the exact nature of similar sources can vary substantially from region to region, and thus the use of different sets of non-specific regional source profiles in a given attribution study can lead to significant differences among receptor model applications (e.g., [19]). Therefore, in an international context, the availability of organic sources profiles data must be extended for areas where no previous information is available.

This work provides an initial data set of organic source profiles based on the chemical characterization of fine OC for 12 major emission source types from five general source categories in the Monterrey Metropolitan Area (MMA). The MMA is the second-most populous urban center in Mexico with air quality problems due to high concentrations of PM₁₀ and PM_{2.5}. It has been estimated that fine OC represents the major fraction of the PM_{2.5} found in the ambient air of the MMA, accounting for 36–71% of the average PM_{2.5} mass [20,21]. The chemical characterization of the ambient fine OC in the MMA has been scarcely studied, focused mainly on PAHs [22,23]. Only one study that included a wide chemical characterization of organic compounds has been conducted [24], which has been also the only source apportionment study based on the organic markers approach conducted in the MMA [24], which is the second of its class in the country after the one reported by Stone et al. [25]. In addition to deriving necessary region-specific organic source profile data for countries with emerging economies, statistical tests were performed to provide insight into the uniqueness of the obtained profiles, thus ensuring source representativeness. The obtained source profiles can be used to conduct source apportionment studies in the MMA or other locations with similar emission sources.

2. Materials and Methods

2.1. Study Area and Sampling

The MMA, the second largest urban center of Mexico, was selected for this study (Figure 1). The potential types of sources that contribute to PM_{2.5} concentrations in the MMA were identified from previous studies [24,26] and official emission inventories [27]. Source samples were collected in June and July of 2014 to represent five general source categories: (1) meat cooking operations, (2) motor vehicle exhausts, (3) open waste burning, (4) industrial emissions, and (5) environmental background.

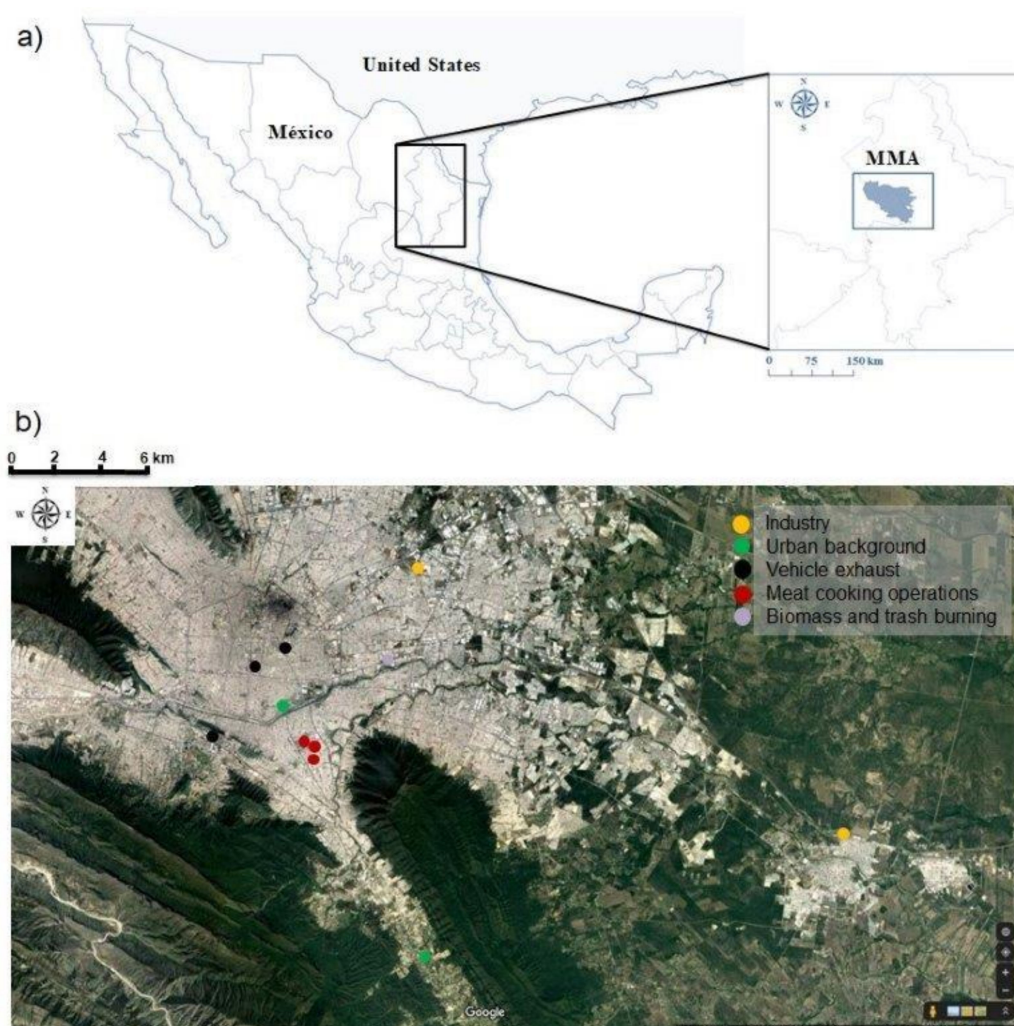


Figure 1. (a) General geographic location of the study area; (b) sampling points for every source profile (source: Google Earth).

A general scheme of the methodology for this study is shown in Figure 2. All the samples were collected on Teflon and quartz fiber filters following a ground-based source-dominated approach for source profile characterization (e.g., [28,29]). Before sampling, Teflon filters were weighted by gravimetry while quartz fiber filters were pre-fired for 8 h at 600 °C in a furnace to remove residual carbon. Teflon and quartz fiber filters were stored in petri-slides and in baked aluminum foil within sealed plastic bags, respectively, until they were used. During the sampling, two filter-based instruments were used in parallel to collect the samples from each source emission. The first one was a MiniVol low-volume sampler (Airmetrics, Springfield, OR, USA; flow rate of 5–7 L/min) to collect samples on 47 mm Teflon filters (Whatman, Maidstone, UK), and the second one was a high-volume sampler (TE-6070-2.5, Tisch Environmental, flow rate of 1100–1200 L/min; Cleves, OH, USA) to collect samples on 20×25 cm micro-quartz filters (Whatman QM-A; Maidstone, UK). The two samplers were calibrated previously to each test by using NIST- traceable certificated orifice calibrators MNF-1236 and TE-5040 for the MiniVol and Hi-Vol samplers (Airmetrics, Springfield, OR, United States), respectively. After sampling, collected filters were placed in a cooler with blue ice for immediate transport from the sampling site to the laboratory. All collected filters were stored at −20 °C in the dark until they were analyzed. The sampling sites for each source category and their descriptions are shown in Table 1.

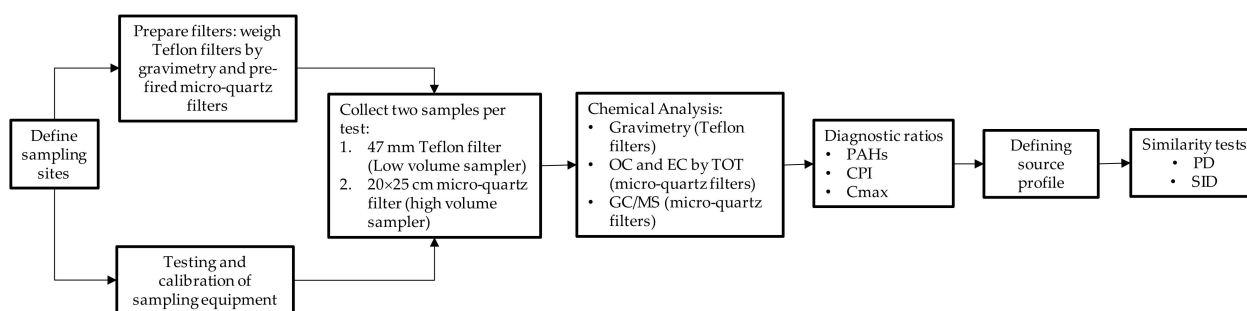


Figure 2. Methodology for the development of organic source profiles.

Table 1. Summary of sampling schemes for the different emission sources.

Source Category	Profile	Sample Code	Number of Samples	Sampling Date	Sampling Time Range (h)
Meat cooking operations	Restaurant charbroiled and grilled meat (25°39'18.9" N, 100°17'29.2" W)	CAR	2	26 June 2014	4.0
	Residential charbroiled meat (25°39'00.5" N, 100°17'05.5" W)	CAF	2	29 June 2014	2.9
	Supermarket charbroiled meat service (25°38'21.7" N, 100°17'00.6" W)	CAS	2	4 June 2014	2.3
Vehicle exhausts	Gasoline-powered vehicles (Loma Larga Tunnel) (25°39'30.25" N, 100°20'11.85" W)	TLL	3	2 July 2014	3.6
	Urban Transport (Av. Juarez, crossing with Arteaga Street) (25°40'59.2" N, 100°18'48.6" W)	TP	3	12 July 2014	3.4
	Freight transport (Av. Felix U. Gomez, crossing with Av. Ciudad Los Angeles) (25°42'28.7" N, 100°16'55.9" W)	CC	3	12 July 2014	2.6
Industry	Oil refinery (25°36'10" N, 99°59'19.7" W)	PMX	2	18 June 2014	12.9
	Manufacturing industry (25°39'30.25" N, 100°20'11.85" W)	PSN	4	25 June 2014	8.0
Biomass and trash burning	Open waste burning (25°41'24.1" N, 100°10'00.1" W)	QB	2	25 June 2014	0.9
Urban background	Suburban area in daytime (25°29'34.1" N, 100°10'52.8" W)	RTD	3	20 June 2014	6.8
	Suburban area in nighttime (25°29'34.1" N, 100°10'52.8" W)	RTN	2	27 June 2014	15.2
	Urban construction site (Av. Felix U. Gomez, Line 3 of the city subway construction site) (25°41'24.1" N, 100°17'47.5" W)	RP	2	4 July 2014	2.2

2.2. Sampling Sites Description

Each sampling site corresponded to a hot spot highly impacted by each source emission type. Preliminary sampling tests were conducted to estimate the proper location and sampling time for each source emission (Table 1) based on the saturation of the filters. A total of 30 individual profile samples were collected and depending on particle loading, the sampling duration varied from 0.9 h for open waste burning to 15.2 h for the suburban area at nighttime.

Meat cooking emissions were collected based on the most common forms of cooking operations in the MMA. These samples included emissions from restaurants that use natural gas for heating (hot plate) purposes and seed oils for food cooking as well as charbroiled meat services at supermarkets and residential charbroiled meat activities. More specifically, the residential cooking test was conducted by cooking a specific combination of meat types and other food complements (e.g., sausage, onions, cheese) using an outdoor charbroiling system. Two samples were obtained for each type of cooking source; all tests involved the cooking of meat from beef, pork, sausage, and other typical food dishes associated with the traditional charbroiled cooking operations in the MMA. Based in both, other references [28,29] and the infrastructure of the cooking operation system, the sampling equipment was positioned at approximately 1.5 m downwind from each source.

Motor vehicle exhaust samples were collected for gasoline- and diesel-powered vehicles from a road tunnel and through side-road sampling, respectively. In both cases, the samplers were placed on a sidewalk close to the traffic lanes, with the sampling inlet placed at 1.5 m above ground level. For the gasoline-powered vehicle emissions, the same site and general procedure described by Mancilla and Mendoza [30] was followed. These samples were collected from a two-bore urban tunnel (532 m long) in which the traffic is composed of 98% gasoline-powered vehicles, most of them light-duty passenger cars. The samplers were located approximately 200 m downstream from the inlet of the north-south bore with a positive slope of 3.5%. The vehicle exhausts for diesel-powered vehicles were divided in two categories: urban (public and private buses) and freight transport (at least four-axle single units and trailers). Information about the main transit routes in the MMA with high urban and freight transport traffic was provided by the Monterrey Department of Public Safety and Roads. From this data, two street locations were selected for sampling these source emissions. Samples were collected during the hours in which the fleet of diesel-powered vehicles was significantly higher (400 buses/h and 200 trailers/h) than other means of transportation (mainly gasoline-powered vehicles); this was determined by previously monitored vehicle count tests in the selected avenues.

The biomass and trash burning profile was obtained by ground-based source-dominated sampling in the plumes of real open-waste burning emissions. The waste burned consisted of wood, grass, leaves, plastics, cardboard, paper, textiles, and household materials. The samples were collected at 2 m downwind from the open fire, where the smoke particles directly impacted the sampler. This procedure was conducted in the suburbs of the MMA, where these types of burnings occur, randomly tracking burning events as they occurred.

The urban background profile was obtained by sampling in a country villa (approximately 60,000 m²) located in the suburban area of the MMA at 30 km southeast from the downtown area, upwind from the urban core with respect to the typical prevailing wind patterns in the region (i.e., east–west). This villa is far from the urban area, thus allowing for the isolation of environmental background emissions. This site is a natural area for recreational purposes (uninhabited), and it is surrounded by shrubs, grass, and woody trees. Sampling was conducted when these activities were not occurring to minimize their influence on the profile. Secondary organic aerosol (SOA) formation due to the photochemical activity of particles produced over natural landscapes can be expected [31]. Samples were collected for daytime and nighttime to identify a possible SOA contribution in the collected samples. The samplers were placed at 4.5 m above the ground on a small structure rooftop.

Industrial profiles were developed for oil refinery and general manufacturing industry emissions. For the oil refinery, two samples were collected from a sampling site located 3 km downwind from the source. The main emissions on this sampling site come from an oil refinery of 7.7 km² that it is composed of more than 30 facilities that process around 110 thousand barrels of petroleum per day to produce mainly gasoline and diesel fuels and other petrochemical products. Another industrial sector was a typical industrial park of the MMA with several manufacturing companies in the field of automotive assembly, electrical appliances, cosmetics, and petrochemical products. Unlike the case for the oil

refinery, the samples were collected from a sampling site located within 1 km downwind from these industrial sources within the industrial park premises.

The urban construction profile was developed by setting up the samplers close to an urban construction area. This area is influenced by particles from paved roads, concrete, and other construction operations of a new subway line for local transportation. Significant fugitive dust emissions occurred from the construction activities: material handling and road-resuspension by local and close-by traffic.

2.3. Sample Analysis

2.3.1. Gravimetry and OC Determination

The loaded Teflon filters were analyzed for mass by gravimetry using a Sartorius ME5 microbalance (Goettingen, Germany) ($\pm 1 \mu\text{g}$) in a weighing chamber with a controlled temperature ($21 \pm 2 \text{ }^\circ\text{C}$) and relative humidity ($35 \pm 5\%$) for 24 h to obtain the total collected particulate matter.

The micro-quartz filters were analyzed for OC and EC by TOT using a Sunset Laboratory thermo-optical carbon analyzer (Model 4L; Tigard, USA) following the NIOSH 5040 guidelines from the US EPA. A standard punch (1.5 cm^2) was extracted from a loaded quartz microfiber filter and placed in an oven using a quartz boat. The oven was initially purged with He. OC was then analyzed over varying time steps between 45 s and 300 s while maintaining an inert atmosphere (pure He). The heating desorbed OC thermally. The evolved OC was catalytically oxidized to CO_2 in a manganese dioxide (MnO_2) oxidizing oven; subsequently, the CO_2 was swept out of the oxidizing oven with the He stream and reduced to CH_4 in a (Ni/firebrick) methanator and quantified as CH_4 by a flame ionization detector (FID). OC was tracked at different temperatures during the specified time frame: $310 \text{ }^\circ\text{C}$, $475 \text{ }^\circ\text{C}$, $615 \text{ }^\circ\text{C}$, and $870 \text{ }^\circ\text{C}$, respectively. The EC analysis was conducted using temperature profiles with a withhold time of 45 s and a final holding time of 120 s at $870 \text{ }^\circ\text{C}$ in an oxidizing atmosphere (He: O_2 90:10 *v/v*). EC was oxidized from the filter into the oxidation oven, converted into CO_2 , reduced to CH_4 , and detected by FID as CH_4 . During this stage, a pyrolysis correction was made. A split point should be defined for OC and EC to quantify these components. The split point is defined as the point at which the light transmittance of the sample returns to the initial value. The carbon that evolved before or after the split point was considered OC or EC, respectively [32].

2.3.2. Organic Markers Characterization

Solvent-extractable organic markers were quantified by GC/MS using dichloromethane (DCM) and methanol (MeOH), both at high purity of $\geq 99.9\%$ (Fischer Scientific Optima grade). Individual filters were cut into pieces and spiked with 50 μL of the following deuterated internal standards (isotopic purity of 98–99 atom % D, Sigma Aldrich): n-hexadecane- d_{34} , n-hexatriacontane- d_{74} , n-eicosane- d_{42} , n-triacontane- d_{62} , n-tetracosane- d_{50} , vanillin- d_3 , benzophenone- d_5 , dibenzo(a,h)anthracene- d_{14} , naphthalene- d_8 , chrysene- d_{12} , benzo(e)pyrene- d_{12} , coronene- d_{12} , 1,4-dichlorobenzene- d_4 , acenaphthylene- d_{10} , perylene- d_{12} , benzaldehyde-2,3,4,5,6- d_5 , decanoic acid- d_{19} , palmitic acid- d_{31} , stearic acid- d_{35} , terephthalic acid- d_4 , levoglucosan- $^{13}\text{C}_6$, cholesterol- d_6 , and 1,4-benzoquinone- d_4 . Thereafter, a DCM extraction was conducted three times. During each extraction, enough DCM was added to fully cover the filters, and then ultrasonic agitation was applied for 20 min using a sonicator (Bransonic[®], 5510R-DTH; Brookfield, CT, USA). The extracts were gathered together and then concentrated by evaporation under a low flow of ultra-high-purity nitrogen until the extract reached a volume of $\sim 5 \text{ mL}$. The extracts were filtered through a pre-fired quartz filter and subsequently reduced in volume using the same flow of high purity nitrogen to obtain a final extract of 250 μL . The extracts were then separated into three fractions with one fraction for a direct analysis by GC/MS, and the other two fractions were used for chemical derivatizations before being introduced to the GC/MS. One derivatization was the methylation using diazomethane (CH_2N_2) to convert carboxylic acids to their respective methyl esters; 50 μL of a CH_2N_2 solution was combined in a vial

with 50 μ L of extract. The other derivatization was silylation using a combination of N,O-bis(trimethylsilyl)trifluoroacetamide (BSTFA) and trimethylchlorosilane (TMCS) to convert sterols and sugars to their respective trimethylsilyl esters; 50 μ L of BSTFA+TMCS (molar ratio 99:1) was combined with 50 μ L of extract. For each derivatization, the mixtures were allowed to react for 3 h at 70 °C.

Finally, the extracts were analyzed by gas chromatography (Agilent 6890N equipment) coupled with a selective mass detector (Agilent 5973 inert). The separation was performed with a non-polar capillary column of 30 m \times 250 μ m \times 0.25 μ m with 5% of methyl-phenyl-siloxane. For each sample, 3 μ L of the extract was supplied to the GC through an automated injector (Agilent 7683 equipment). The operating conditions of the GC/MS began with a temperature of 65 °C for the first 5 min, and then the temperature increased at a rate of 10 °C/min for 25 min until the GC oven reached a temperature of 300 °C. The quantification and identification of the organic compounds were based on comparisons with authentic standards, retention times, literature mass spectra, and fragmentation patterns using the HP ChemStation software. The full list of organic compounds to be identified and quantified is showed in Table 2. A scheme of the GC/MS methodology is shown in Figure 3 and more details of the extraction and chemical analysis process of the organic markers can be found elsewhere [33].

Table 2. List of the extractable organic compounds for this study.

Label	<i>n</i> -alkanes	Label	Hopanes	Label	<i>n</i> -alkanoic acids
C19	n-nonadecane	HOP1	18a(H)-22,29,30 trisnorneohopane	C10-Acid	n-Decanoic acid
C20	n-eicosane	HOP2	17a(H)-22,29,30-trisnorhopane	C11-Acid	n-Undecanoic acid
C21	n-henicosane	HOP3	17a21b-29hopane	C12-Acid	n-Dodecanoic acid
C22	n-docosane	HOP4	18a(H)-30-Norneohopane	C13-Acid	n-Tridecanoic acid
C23	n-tricosane	HOP5	17a21b-hopane	C14-Acid	n-Tetradecanoic acid
C24	n-tetracosane	HOP6	22S 17a21b-30-homohopane	C15-Acid	n-Pentadecanoic acid
C25	n-pentacosane	HOP7	22R 17a21b-30-homohopane	C16-Acid	n-Hexadecanoic acid
C26	n-hexacosane	HOP8	22S-17a21b-30-bishomohopane	C17-Acid	n-Heptadecanoic acid
C27	n-heptacosane	HOP9	22R-17a21b-30-bishomohopane	C18-Acid	n-Octadecanoic acid
C28	n-octacosane			C19-Acid	n-Nonadecanoic acid
C29	n-nonacosane	Label	Methoxyphenols	C20-Acid	n-Eicosanoic acid
C30	n-triacontane	GUA	Guaiacol	C21-Acid	n-Henicosanoic acid
C31	n-hentriacontane	MGUA	4-Methylguaiaicol (2-methoxy-4-methylphenol)	C22-Acid	n-Docosanoic acid
C32	n-dotriacontane	MSYR	4-Methylsyringol (2,6-dimethoxy-4-methylphenol)	C23-Acid	n-Tricosanoic acid
C33	n-tritriacontane	SYA	Syringaldehyde Vanillin	C24-Acid	n-Tetracosanoic acid
C34	n-tetratriacontane	VAN	(4-hydroxy-3-methoxy benzoic acid)	C25-Acid	n-Pentacosanoic acid
Label	PAH	IVAN	Isovanillin (3-hydroxy-4-methoxybenzaldehyde)	C26-Acid	n-Hexacosanoic acid
FLT	Fluoranthene	Label	Resin acids	C27-Acid	n-Heptacosanoic acid
ACE	Acephenanthrylene	AB-Acid	Abietic acid	C29-Acid	n-Nonacosanoic acid
PYR	Pyrene	DHAB-Acid	Dehydroabietic acid		
BaA	Benzo(a)anthracene	ODHAB-Acid	7-Oxo-dehydroabietic acid		
CHR	Chrysene	PIM-Acid	Pimaric acid		
BbF	Benzo(b)fluoranthene	IPIM-Acid	Isopimaric acid		
BaP+BeP	Benzo(a)pyrene + Benzo(e)pyrene	Label	Other acids		
PER	Perylene	CPIN-Acid	cis-Pinonic acid		
IPY	Indeno (1,2,3-cd)pyrene	OLE-Acid	cis-9-octadecenoic acid (Oleic acid)-C18		
BPE	Benzo(g,h,i)perylene		Sugars		
DaA	Dibenzo(a,h)anthracene	LEV	Levogluconan		
COR	Coronene		Sterols		
RET	Retene	CHO	Cholesterol		

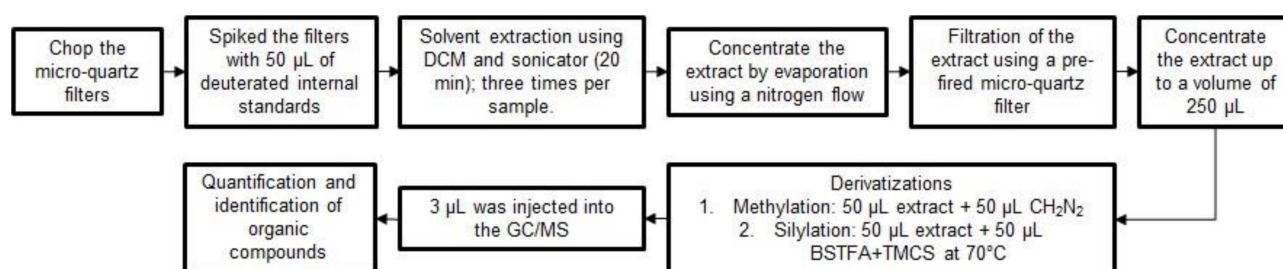


Figure 3. General methodology for conducting the GC/MS analysis.

2.4. Source Profile Representativeness

Near-field source sampling has the benefit of providing an average source composition of evolved emissions from a target upwind source. As can be seen in other studies, representativeness with low number of samples can be achieved following a ground-based source-dominated approach for source profile characterization [28,29]. A well-known example of this is the use of roadway tunnels to characterize overall emissions from a vehicle fleet. This is particularly useful when the goal is not to characterize each individual vehicle but rather to obtain a representation of the fleet; however, a known drawback of this approach is that other upwind or background sources will be part of the sampled air masses. In addition, the sample will be a mix of emissions from the major source being targeted and a set of minor sources that occur at the same time that are complicated to eliminate due to the real-world condition of the sampling. Thus, it is convenient to know how well the derived emission profiles represent the target sources. To do so, in this study, we opted to estimate diagnostic ratios to obtain a representation of the most probable origin of the emissions and similarity metrics to establish a degree of uniqueness. In addition, Table 3 summarizes the main organic markers used to distinguish between source profiles.

Table 3. Key organic markers for every source profile.

Emission Source Profile	Organic Marker
Restaurant charbroiled and grilled meat	Cholesterol and levoglucosan
Residential charbroiled meat	Cholesterol and levoglucosan
Supermarket charbroiled meat service	Cholesterol and levoglucosan
Gasoline-powered vehicles	High molecular weight PAHs and n-alkanes
Urban transport	Low molecular weight PAHs, n-alkanes and hopanes
Freight transport	Low molecular weight PAHs, n-alkanes and hopanes
Oil refinery	Hopanes and n-alkanes
Manufacturing industry	Hopanes and n-alkanes
Open waste burning	Levoglucosan, methoxyphenols and diterpenoids
Suburban area in daytime	Cis-pinonic acid (secondary organic marker)
Suburban area in nighttime	Cis-pinonic acid (secondary organic marker)
Urban construction site	Hopanes and n-alkanes

2.4.1. Carbon Number Indicators

Carbon number indicators are useful to identify whether a given emission profile is from natural or anthropogenic sources. The carbon preference index (CPI) is an indicator of the measure of odd- or even-carbon homologue series of organic compounds within a sample. Based on several studies [34–38], the CPI for n-alkanes (odd to even ratio) was calculated as:

$$CPI = \frac{C_{17} + C_{19} + C_{21} + \dots + C_{33}}{C_{16} + C_{18} + C_{20} + \dots + C_{32}} = \frac{\sum(C_{17} \text{ to } C_{33})_{odd}}{\sum(C_{16} \text{ to } C_{32})_{even}} \quad (1)$$

and that for *n*-alkanoic acids (even to odd ratio) as:

$$CPI = \frac{C_{10} + C_{12} + C_{14} + \dots + C_{32}}{C_{11} + C_{13} + C_{15} + \dots + C_{31}} = \frac{\sum(C_{10} \text{ to } C_{32})_{\text{even}}}{\sum(C_{11} \text{ to } C_{31})_{\text{odd}}} \quad (2)$$

For both *n*-alkanes and *n*-alkanoic acids, high values of CPI (> 5) indicate that they are emitted from natural sources (e.g., plant waxes), whereas values of CPI close to the unity indicate that they are emitted from anthropogenic sources [38–44].

Another useful indicator that is used to identify the origin of the emissions is the highest carbon number among the homologous series (C_{max}). For *n*-alkanes and *n*-alkanoic acids, a high molecular weight (> C_{25} and > C_{20} , respectively) is emitted from biogenic sources, while those with a low molecular weight ($\leq C_{25}$ and $\leq C_{20}$, respectively) are mainly emitted from fossil fuel combustion processes and meat cooking operations [37,39,41,45]. The information provided by these indicators is valuable as it can be used to provide an initial insight into how well the sampling process was able to capture the target emission sources.

2.4.2. PAHs Ratios

The PAH diagnostic ratios can be used to recognize—with an additional level of detail—the origin of the emission sources [36,44,46–52]. For the present work, the diagnostic ratios estimated for each organic profile are shown in Table 4. Characteristic values for these ratios can be found elsewhere [43,48,53–58].

Table 4. Diagnostic ratio ranges for PAH from different source types.

Diagnostic Ratio *	Range	Source Type
IPY/(IPY+BPE)	<0.20	Petrogenic
	>0.20	Pyrogenic
	0.20–0.50	Petroleum combustion
	>0.50	Coal, grass, and wood combustion
FLT/(FLT+PYR)	<0.40	Petrogenic
	>0.40	Pyrogenic
	0.40–0.50	Fuel combustion
	>0.50	Diesel combustion
BaA/(BaA+CHR)	<0.20	Petrogenic
	0.20–0.35	Coal combustion
	>0.35	Pyrogenic, vehicle exhausts

* PAHs abbreviations are defined in Table 2.

2.4.3. Test of Similarity between Organic Source Profiles

Similarities between different organic source profiles can be identified using the Pearson distance (PD) and the similarity identity distance (SID) in accordance with Belis and Pernigotti [59]. PD is equal to $1 - r^2$, where r^2 is the Pearson coefficient, and SID is defined by equation (3) [60]:

$$SID = \frac{\sqrt{2}}{m} \sum_{j=1}^m \frac{|x_j - y_j|}{x_j + y_j} \quad (3)$$

where x_j and y_j are the relative masses of organic marker j to the $PM_{2.5}$ of two different organic source profiles (x and y), and m is the number of common organic compounds between these profiles. These two metrics (PD and SID) aim to compare two profiles based on their common chemical relative mass composition. PD is highly sensitive to variations in the major components of $PM_{2.5}$, while SID is evenly sensitive to all components [60]. $PD < 0.4$ and $SID < 0.8$ are acceptable criteria for profile similarity [60]. Several researchers have successfully used this approach to assess the similarity among source emission profiles [59,61].

To complement this statistical analysis, a coefficient of divergence (COD) analysis was conducted. CODs are used to determine the relative measure of homogeneity or spatial variability in the concentration fields of any pollutant [62], while others have used it to find similarities between source profiles [58]. The COD is defined as follows, Equation (4):

$$COD_{jk} = \sqrt{\frac{1}{p} \sum_{i=1}^p [(z_{ij} - z_{ik}) / (z_{ij} + z_{ik})]^2} \quad (4)$$

where z_{ij} and z_{ik} are in this case the average mass concentration or fraction of chemical species i for source emission profiles j and k , and p is the number of chemical species. Values of CODs near the unity indicate that profiles j and k are different, and as the values approach zero, it indicates that profiles j and k are similar.

3. Results and Discussion

3.1. General Results

Based on the detailed organic characterization for each sample obtained, 12 average source profiles were derived (Table S1 of the Supplementary Material). The total extractable organic matter (EOM) accounted for 6% to 32% of the OC (Figure 4). Depending on the type of emission source, the distribution of % of EOM within each profile can vary. The n -alkanes contribution to the % of EOM varied from 0.5% to 1.0% for meat-cooking operations profiles, from 3.4% to 5.0% for diesel vehicle exhaust, from 1.4 to 4.7 for industry profiles, and about 47% for gasoline vehicle exhaust. The n -alkanes contribution to the total EOM was the highest in the gasoline-powered vehicles profile (TLL) with a contribution that was 9–13 times higher than that of the diesel-powered vehicle exhaust profiles (TP, CC). The hopanes comprised from not detectable to 1.3% of the total EOM, once again being the TLL, CC and TP profiles with the highest hopanes relative contribution to the EOM with values of 0.2%, 0.3% and 1.3%, respectively. The hopanes contribution to the total EOM was also 4–5 times higher for the gasoline-powered vehicles than that observed for diesel-powered vehicles. The PAHs comprised from 0.1% to 1.5% of the EOM. As in the case of the hopanes, the contribution of the PAHs to the EOM was the highest in the gasoline vehicles profile and was 5–6 times higher than that of the diesel vehicles. The total n -alkanoic acids and the sugars (levoglucosan) were the major components among source profiles, accounting from 6.3% to 76% and from 18% to 80% of the EOM, respectively, with large variations among profiles. Five methoxyphenols were quantified comprising 2.5% of the EOM, while sterols (cholesterol) comprised 0.01% to 0.53% of the EOM. The biomass/trash burning profile (QB) had the highest levoglucosan, methoxyphenols, and resin acids relative contribution to the EOM, while the meat cooking operations profiles had the highest sterols (cholesterol) relative contribution to the EOM among all profiles (>0.1%).

The profiles were further processed to obtain the corresponding diagnostic ratios (Table 5). The profiles and diagnostic ratios are discussed in the following sections by major chemical families.

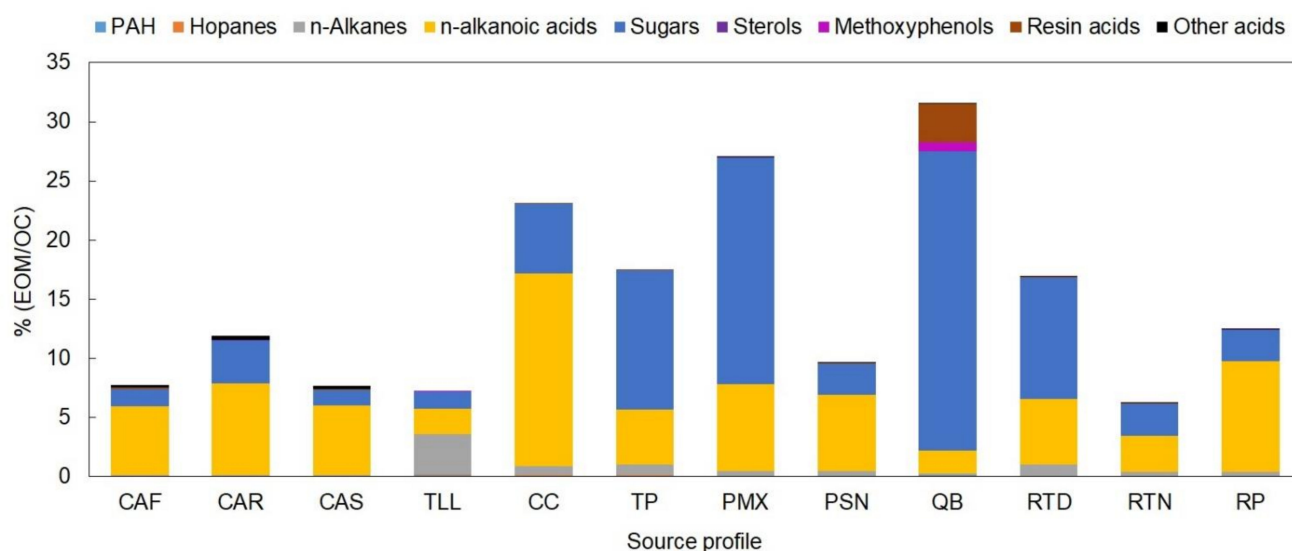


Figure 4. Quantified EOM mass levels of each family of organic compounds in the total OC of each source emission profile. Definition of source profile codes are presented in Table 1.

Table 5. Carbon preference index and diagnostic PAH ratios for each emission source profile.

Profiles	<i>n</i> -alkanes		<i>n</i> -alkanoic Acid		PAHs		
	CPI	C _{max}	CPI	C _{max}	FLT/(FLT+PYR)	IPY/(IPY+BPE)	BaA/(BaA+CHR)
CAF	1.7	C ₂₇	3.6	C ₁₄	0.64	0.60	0.10
CAR	1.7	C ₂₉	2.7	C ₁₅	0.94	0.23	0.84
CAS	1.1	C ₂₄	3.1	C ₁₄	0.63	0.42	0.04
TLL	1.1	C ₂₅	5.6	C ₁₆	0.80	0.45	0.54
CC	1.0	C ₂₅	12.8	C ₁₆	0.73	0.33	0.25
TP	1.1	C ₂₈	3.0	C ₁₆	0.53	0.23	0.20
PMX	1.2	C ₂₄	5.4	C ₁₆	0.97	NA ¹	0.52
PSN	1.0	C ₂₈	4.8	C ₁₆	0.50	0.47	1.00
QB	1.2	C ₂₇	4.5	C ₁₆	0.64	0.57	0.05
RTD	1.2	C ₂₈	4.2	C ₁₆	0.57	0.43	1.00
RTN	1.2	C ₂₉	3.8	C ₁₄	0.75	0.54	1.00
RP	1.0	C ₂₅	17.1	C ₁₆	0.72	0.19	0.16

¹ Not available.

3.2. *n*-alkanes and Hopanes

As can be observed in Figure 5a, the highest *n*-alkanes levels were exhibited on average by the vehicle exhaust profiles (TLL, CC, TP) followed by industry emission profiles (PSN, PMX), which ranged from 1400 to 6700 ng/mg and 880 to 1070 ng/mg, respectively. This is consistent with the fact that *n*-alkanes are derived from petroleum lubricants and fossil fuel combustion processes [15,63–65]. Within the vehicle exhaust profiles, the *n*-alkanes levels for the gasoline-powered vehicle profile (TLL) were two and four times higher than those from diesel-powered vehicles of urban (TP) and freight (CC) transport, respectively. For the manufacturing industry profile (PSN), the *n*-alkanes mass levels were 20% higher than those of the oil-refinery profile (PMX). This could suggest that manufacturing processes are highly dominated by fossil fuel combustion processes. The meat cooking operations profiles exhibited the lowest levels of *n*-alkanes, while the background profiles had *n*-alkanes levels that were on average 20% lower than the industry profiles.

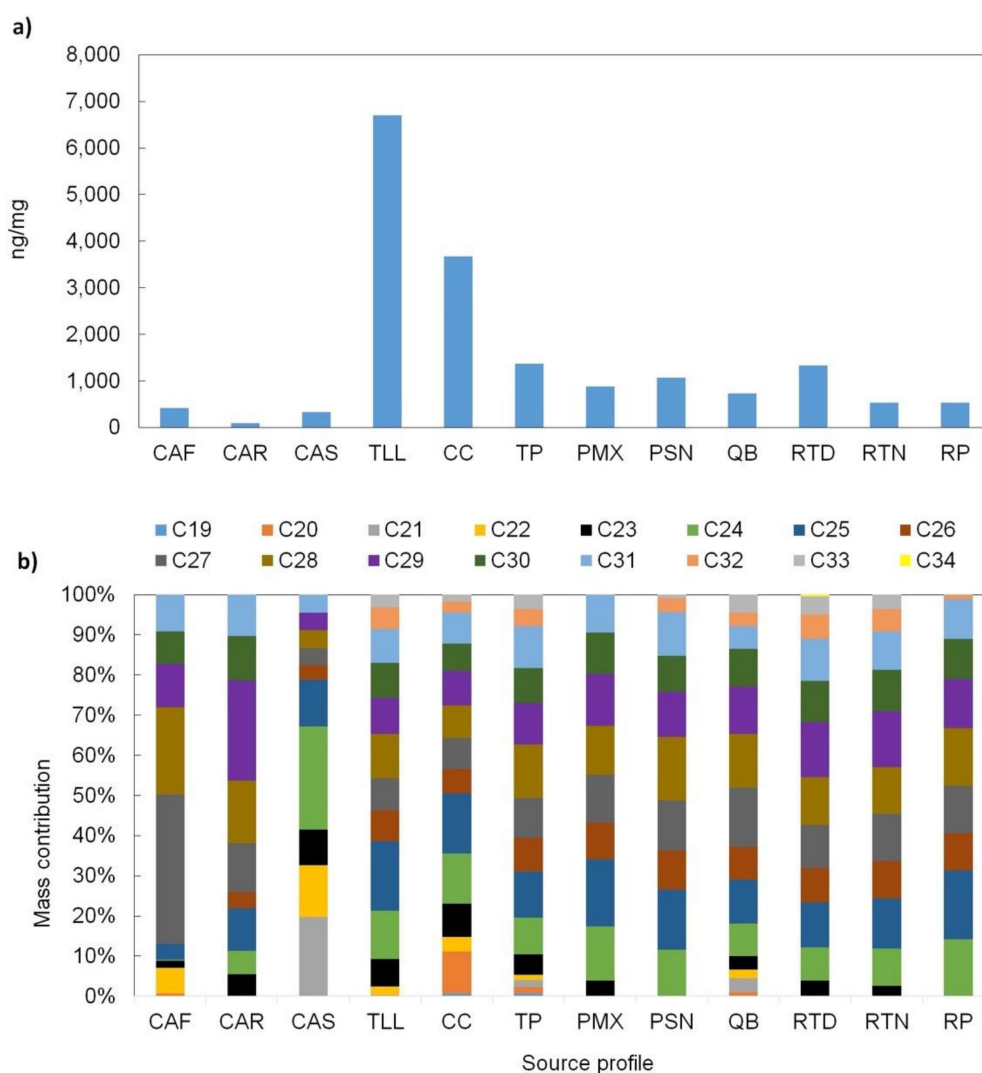


Figure 5. (a) *n*-alkanes total concentration and (b) mass contribution of individual *n*-alkanes to the total *n*-alkanes EOM for each source profile. Definition of source profile codes are presented in Table 1.

To assess whether the organic source profiles were anthropogenic or biogenic in origin, a CPI was calculated for C₁₉ to C₃₃ for each profile (Table 4). The *n*-alkanes had CPI values ranging from 1.0 to 1.7. Overall profiles exhibited values close to the unity, indicating a dominance of anthropogenic sources [41,42]. Only the restaurant charbroiled grilled meat (CAR) and residential charbroiled meat (CAF) profiles had the highest values of 1.7 and 1.7, respectively, consistent with the origin of the fuel and suggesting a slight contribution from natural vegetation waxes [45,66], which consist of long chain plant lipids (>C₂₀) mainly as *n*-alkanes, *n*-alkanoic acids, and *n*-alkanols [67,68]. Similarities among the carbon contribution among vehicle, industry, and background profiles can be observed in Figure 5b along with differences among meat cooking operations with respect to all other profiles. CPI values reported by other researchers were 1.0 [69], 1.1 [69], 1.5 [70] and 2 [58] for gasoline, diesel, wood burning and cooking operations, respectively. All CPI values are close to unity although small differences exist, depending on the particular conditions.

High molecular weight *n*-alkanes (HMW; >C₂₅) primarily originate from plant waxes, for which C₂₇, C₂₉, C₃₁, and C₃₃ are major species [71]. Lower molecular weight *n*-alkanes (LMW; ≤C₂₅) are usually related to anthropogenic activities, such as fossil fuel combustion [42]. The C_{max} for *n*-alkanes varied among source profiles (Table 4). For the restaurant charbroiled grilled meat (CAR), residential charbroiled meat (CAF), open-waste burning (QB) and suburban background (RTD and RTN), the C_{max} were in the range from C₂₇ to C₂₉;

this indicates that these profiles are influenced by biomass burning processes, including some plant waxes, which can emit HMW *n*-alkanes [70,72]. For all other developed source profiles, the C_{max} was dominated by a LMW *n*-alkanes series, suggesting anthropogenic emission sources. For instance, C_{24} , C_{25} , and C_{28} were the C_{max} for TLL, CC, and TP, respectively; this is different from Cai et al. [69], who found that C_{17} was a C_{max} for both gasoline and diesel motor vehicles.

Similarly, the hopanes were detectable for the vehicle exhaust and industry emissions profiles with levels that range from 80 to 240 ng/mg and 31–130 ng/mg, respectively (Figure 6a). Hopanes, which are markers of the petroleum components, are found in lubricant oils employed in motor vehicles and petrochemical industries [15,65]. The total hopanes levels in this study were 83% (TLL) and 66% (TP) lower than those for gasoline- and diesel-motor vehicles reported by Cai et al. [69], respectively.

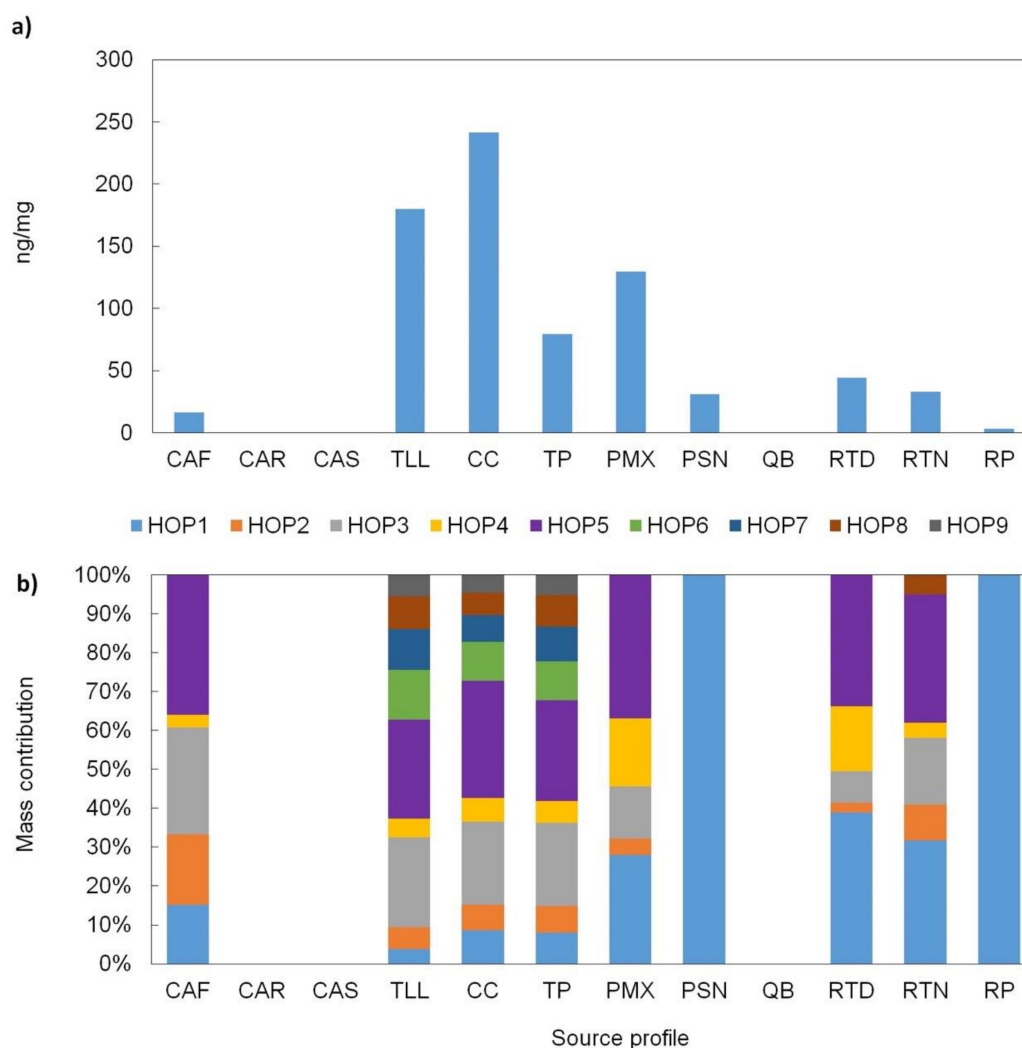


Figure 6. (a) Hopanes total concentration and (b) mass contribution of individual hopanes to the total hopanes EOM for each source profile. Definition of source profile codes are presented in Table 1.

The vehicle profiles showed a full distribution of the hopanes series (HOP1 to HOP9 as defined in Table 2); the hopane with the highest mass contribution was HOP5 (Figure 6b), which has been used as a tracer for vehicle emissions [73]. For the industrial emissions, the PMX profile presented the presence of hopanes in the series HOP1 to HOP5, whereas the PSN profile only exhibited HOP1 (Figure 4); the emissions for PMX were 4.3 times higher than those from the manufacturing industries. Other source profiles had low levels of hopanes. The observed levels in the CAF profile can be associated with the lubricant oils

used to burn the charcoal, while those in the RTN and RTD profiles could be associated with the motor vehicle exhausts from suburban highways and roadways near the site.

3.3. Polycyclic Aromatic Hydrocarbons (PAHs)

PAHs are semi-volatile and ubiquitous organic compounds formed from an incomplete combustion of any organic material. Biogenic sources include forest fires [74,75], and anthropogenic sources comprise emissions from industries, vehicle exhausts, and the combustion of fossil and biomass fuels [46,64,76]. In addition, some are well-known human carcinogens [77], and they can be classified as low molecular weight (LMW; ≤ 4 rings) or high molecular weight (HMW; >4 rings) PAHs. The levels of 13 measured PAHs for each organic source profile are shown in Figure 7a. Retene (RET), an organic marker of conifer wood combustion [78], was detected only in the open waste burning (QB) profile, whereas all other PAHs were detected in several profiles (Figure 7b). The individual PAHs ranged from 0.02 to 318 ng/mg, with chrysene (CHR) having the highest levels among profiles. The total PAHs levels (Σ PAHs) ranged from 1.3 to 522 ng/mg; the suburban profiles showed the lowest Σ PAHs, while the open waste burning and meat cooking operations profiles had the highest levels.

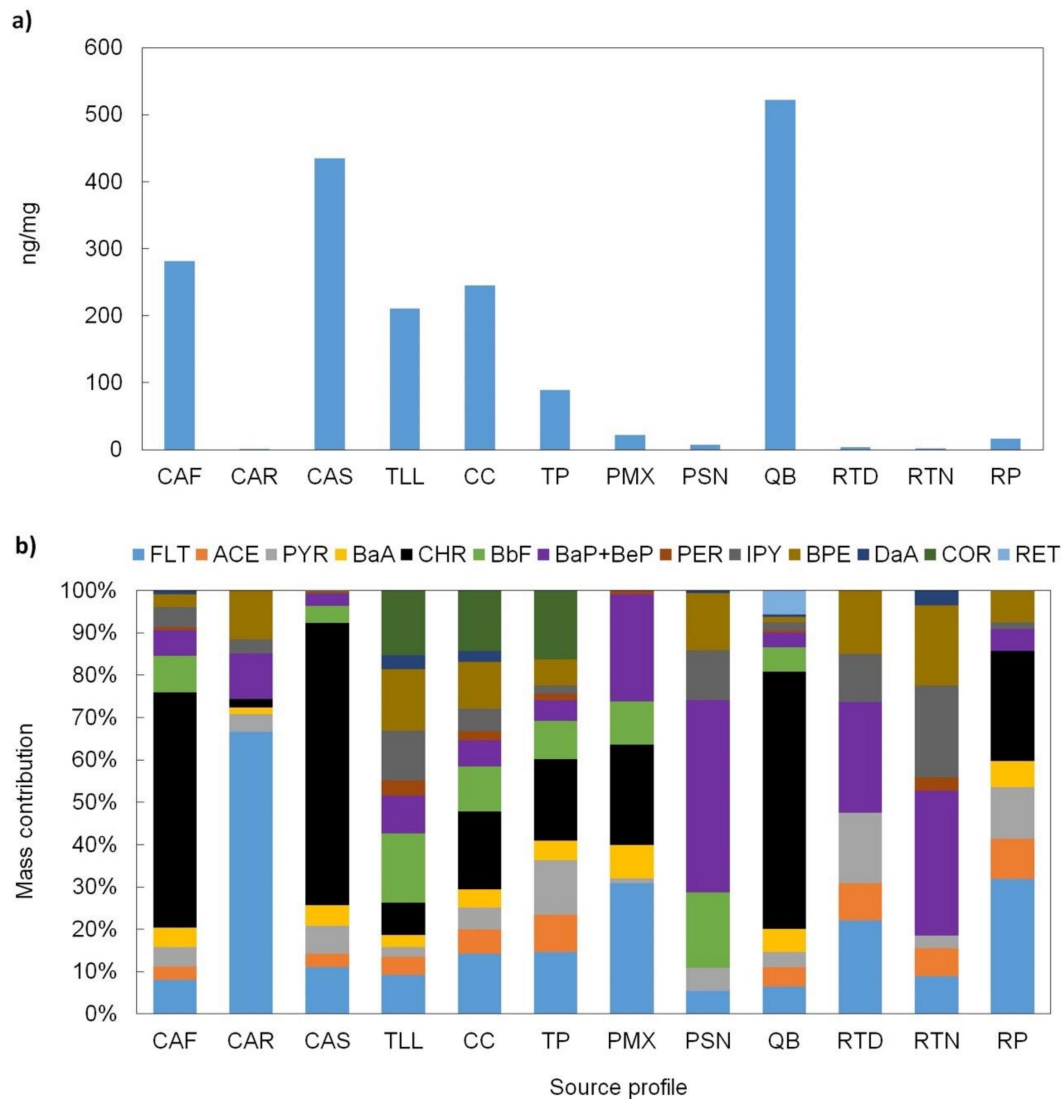


Figure 7. (a) PAHs total concentration and (b) mass contribution of individual PAHs to the total PAH EOM for each source profile. Definition of source profile codes are presented in Table 1.

For the gasoline-powered vehicle profile, the LMW- Σ PAHs were 25% lower than HMW- Σ PAHs. Conversely, for the diesel-powered vehicle profiles, LMW- Σ PAHs were 1.4–2.3 times higher than HMW- Σ PAHs. This is characteristic in differentiating between gasoline- from diesel-powered vehicles [52,69,79]. For both, gasoline- and diesel-powered vehicle profiles, the major component for LMW- Σ PAHs was chrysene, while for HMW- Σ PAHs, it was coronene. The latter is partially different from that found by other studies in which pyrene and coronene were reported as the major components for gasoline-powered vehicles [69,80], while for diesel-powered vehicles, the major components that were reported are pyrene and benzo(ghi)fluoranthene [69,81].

The meat cooking operations and open-waste burning profiles were dominated by LMW- Σ PAHs, which were 3, 6, 26, and 7 times higher than those of HMW- Σ PAHs in CAR, CAF, CAS, and QB, respectively. The CAF, CAS, and QB profiles had chrysene as the major component, while for the CAR profile, fluoranthene and pyrene were major components. This suggests that CAF, CAS, and QB operations utilized charcoal and organic matter derived from hardwoods [70], while CAR operations can be associated with operations that use seed oils for cooking food [79] and natural gas for heating [82].

Characteristic diagnostic ratios for PAHs are shown in Table 4. The range values for FLT/(FLT+PYR) were from 0.50 to 1.0. For IPY/(IPY+BPE), they were 0.19–0.60, and for BaA/(BaA+CHR), they were 0.04–1.0. These ratios can be used to suggest the source origin of the organic profiles. The values of these ratios for meat cooking operations (CAF, CAR, and CAS) and vehicle exhaust (TLL, CC, and TP) indicate pyrogenic sources, such as charcoal combustion and fossil fuel combustion, respectively. For the industry emissions (PMX and PSN), the ratios could be associated with the presence of petcoke processes (pyrogenic source) within the oil-refinery profile, whereas for the manufacturing industry, they indicate a dominance of fuel combustion processes. The latter is in line with the low levels of hopanes exhibited by the manufacturing industry compared with oil-refinery emissions. For open waste burning (QB), the ratios indicate grass and wood combustion. Finally, for suburban profiles, the values of these ratios suggest a mixture of biomass burning, fossil fuel, and fuel oil combustion processes based on the results obtained in other studies [43,48,53,56]. For instance, Chen et al. [49] reported BaA/(BaA+CHR) ratios of 0.22–0.55 and 0.38–0.65 for gasoline and diesel motor vehicles, respectively, while Alves et al. [50] reported FLT/(FLT+PYR), IPY/(IPY+BPE), and BaA/(BaA+CHR) values of 0.23, 0.37, and 0.75, respectively. In this study, the corresponding ratios were different than those from these studies, suggesting differences in traffic fleet characteristics (e.g., age, car model, maintenance, fuel quality) among regions.

3.4. *n*-alkanoic Acids

The *n*-alkanoic acids are ubiquitous, and they are commonly used as complementary organic markers. It can be observed that overall source profiles in this study are acid-enriched. The total levels of these acids ranged from 4156 ng/mg to 75,311 ng/mg (Figure 8a). Most of the relative contribution of *n*-alkanoic acids is comprised of C₁₄–C₁₈ acids (Figure 8b), suggesting an attribution to anthropogenic sources [83]. The CPI for *n*-alkanoic acids ranged from 2.7–17, and the C_{max} for *n*-alkanoic acids was in the range from C₁₄ to C₁₈, indicating an anthropogenic origin [83]. For some organic source profiles, such as meat operations and environmental background profiles, a low contribution of *n*-alkanoic acids > C₂₀ indicated a contribution from plant waxes [83]. Another marker detected, particularly in the meat cooking operations profiles, was oleic acid, which is related to the oils used in cooking; the concentrations of this acid were 84–98% lower than the levels reported by Zhao et al. [84] and Schauer et al. [85]. These low levels suggest the use of low-quality oils given that oleic acid is found in natural oils of high quality (e.g., olive oil, avocado oil).

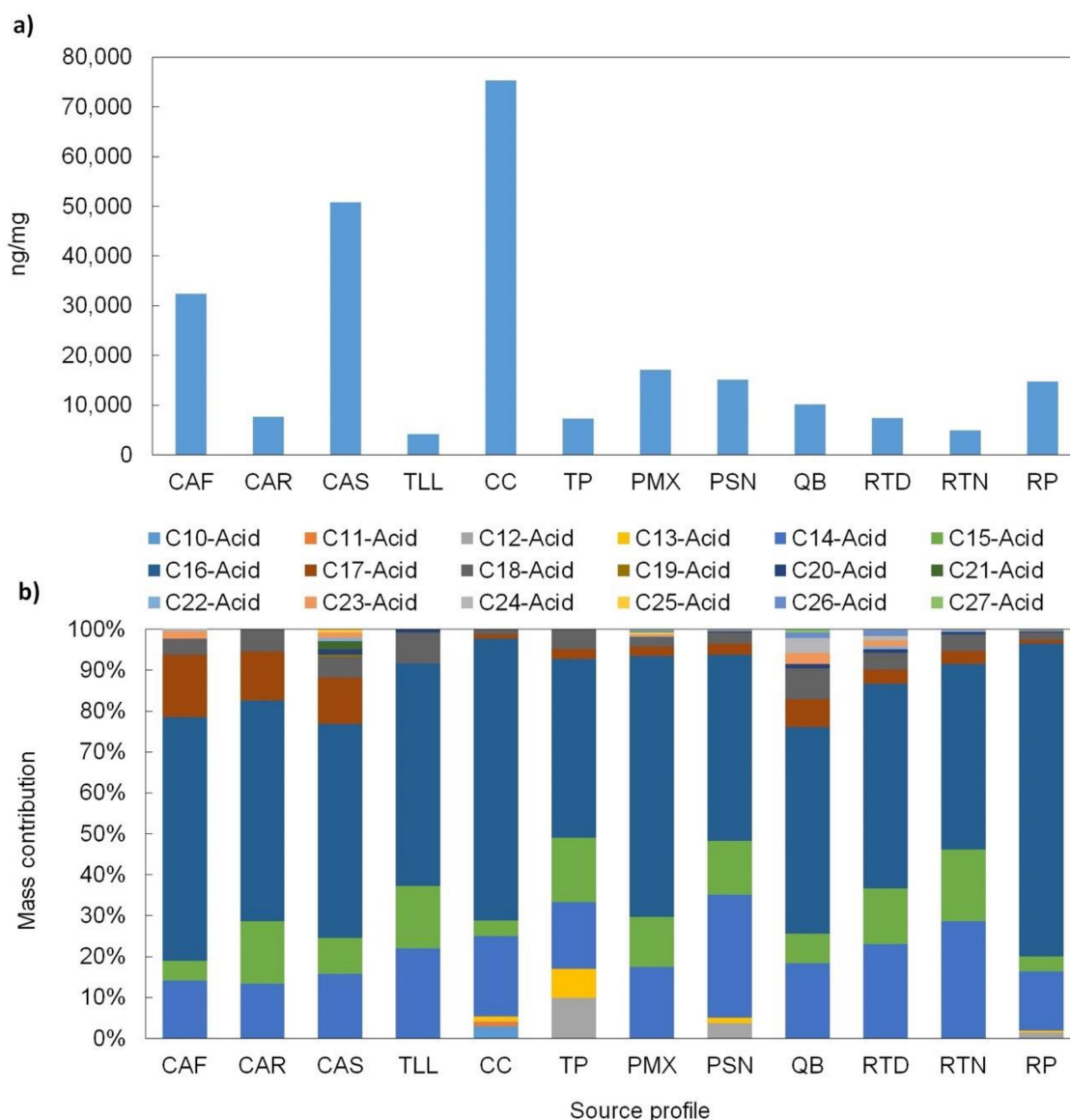


Figure 8. (a) *n*-alkanoic acids total concentration and (b) mass contribution of individual *n*-alkanoic acids to the total *n*-alkanoic acids EOM for each source profile. Definition of source profile codes are presented in Table 1.

3.5. Levoglucosan and Cholesterol

The major organic marker for smoke particles from biomass burning is levoglucosan, which is derived from the thermal decomposition of cellulose and lignin [70,86–90]. For steroids, cholesterol has been used as a good marker for meat-cooking operations, specifically for particles emitted directly from meat when being cooked [85,91,92].

The average abundances for levoglucosan and cholesterol can be observed in Figure 9. Their levels ranged from 2920 to 130,000 ng/mg for levoglucosan and 3.7 to 81 ng/mg for cholesterol. The open waste burning profile (QB) is clearly dominated by levoglucosan, whose levels are 3 to 45 times higher than those from the other profiles. In addition, the levoglucosan concentration was 7.5 and 94 times higher than the concentration reported by Wang et al. [93] and Schauer et al. [70], respectively. These differences can be attributed to the uniqueness of the profiles. For example, for the QB profile, the biomass burning was an uncontrolled open fire with a combination of different waste materials, whereas for both Wang et al. [93] and Schauer et al. [70], profiles were obtained from a controlled domestic fireplace burning only wood. For the meat cooking operations profiles, the cholesterol was the major component with levels 4 to 20 times greater than those from the other

profiles. These profiles showed relatively low levels of levoglucosan from the combustion of charcoal [94], while the cholesterol was from meat cooking [85]. The levoglucosan for CAS and CAF was 3 and 2 times higher than the levels in the CAR profile, respectively; this could be associated with the fact that restaurants use less charcoal and also use natural gas for cooking operations. The cholesterol for the CAR profile was 21% lower than in the CAS and CAF profiles; this could suggest that restaurants cook not only meat but also other meals with a low content of cholesterol. The cholesterol concentrations in this study were ~90% and ~98% lower than those reported by Zhao et al. [83] and Schauer et al. [85], respectively. Finally, the CC, TP, and PMX profiles exhibited a presence of levoglucosan, suggesting a slight influence from background biomass burning emissions.

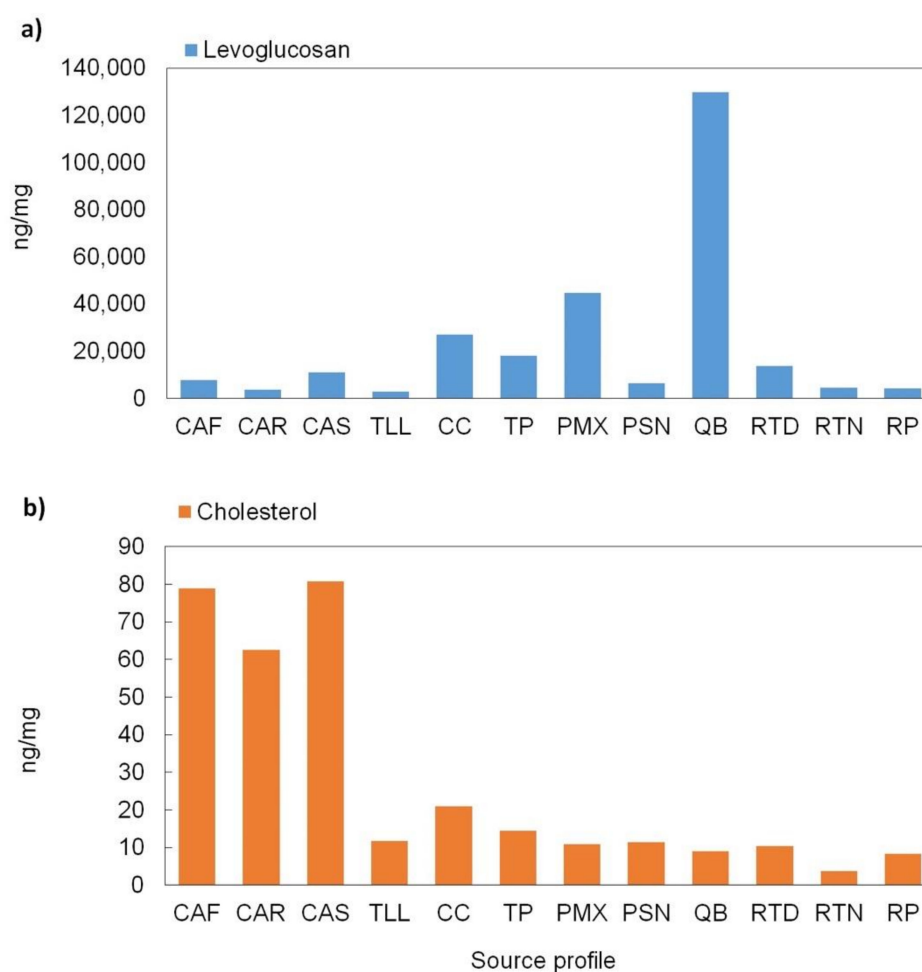


Figure 9. Levels of levoglucosan (a) and cholesterol (b) in the individual profiles.

3.6. Methoxyphenols

Lignin is a key organic polymer present in vascular plants, particularly in wood and bark. It produces phenolic markers when these biomasses are burnt [66,95–97]. The open waste burning profile (QB) was the only profile in which the methoxyphenols were detectable with a total level of 4115 ng/mg. Five methoxyphenols were quantified. Vanillin, isovanillin, and guaiacol constituted 25% of the total methoxyphenols identified, suggesting the combustion of softwood, such as pine wood or other conifers, while the 4-methylsyringol and syringe aldehyde constitute the remaining 75%, indicating the combustion of hardwoods [98,99].

3.7. Resin Acids (Diterpenoids)

Resin acids are produced by some wood species (e.g., conifers), and they can be released when the wood is burned or degraded [100]. These organic markers are typically used to distinguish between softwood and hardwood combustion [70,101]. The pimaric and isopimaric acids are natural product resin acids along with abietic acid, whereas dehydroabietic acid and retene are secondary organic markers. All are used as organic markers for softwood burning [100,102]. These organic compounds occurred in the open waste burning profile (QB) with a contribution of 16,467 ng/mg, comprising 10% of the EOM. The presence of these organic markers suggests that most of the smoke particles in this profile were from softwood burning. In addition, the relatively high level of dehydroabietic acid (4497 ng/mg) compared with that of abietic acids (6906 ng/mg) indicates that smoke particles are rapidly degraded. The abietic, dehydroabietic, pimaric, and isopimaric acid levels in this study were 37, 31, 189, and 19 times higher, respectively, than the levels reported by Schauer et al. [70].

3.8. Secondary Organic Markers

The presence of cis-pinonic acid in the manufacturing emissions (PSN) and suburban area (RTD and RTN) and urban construction (RP) profiles suggests the presence of SOA in the samples [103]. The cis-pinonic acid is involved in SOA formation from α -pinene and ozone photoreaction [104,105]. For the RTD and RTN profiles, the presence of cis-pinonic could be associated with a transport emission effect because the collection of samples was carried out during no anthropogenic activity on site. The SOA contribution appears to be higher at nighttime (cis-pinonic contribution was twice of that found in the daytime samples). This could be explained by a transport effect enhanced by a lower mixing height at night, as was found in a previous study by Mancilla et al. [20]. For the PSN, PMX, and RP, the influence of SOA can be explained by the fact that the sampling was carried out in an open area; therefore, background ambient air masses could contribute to SOA [83,106].

3.9. Source Profile Similarity Analysis

All organic source profiles showed distinguishable organic markers. The meat cooking operations were distinguished by cholesterol and levoglucosan. Cholesterol was a characteristic organic marker for emissions from meat itself when cooked and levoglucosan for the smoke particles from charcoal combustion. Vehicle exhausts have hopanes (HOP1 to HOP9) as characteristic organic markers. In addition, heavy-duty diesel truck emissions (urban and freight transport) exhibited higher levels of hopanes and LMW- Σ PAHs than gasoline motor vehicles. The open waste burning was dominated by methoxyphenols and levoglucosan, whereas the urban background was influenced by SOA precursor (α -pinene), as indicated by the presence of cis-pinonic acid. These differences were supported by the results from the similarity tests between the source profiles in this study that can be observed in Figure 10.

The profiles were compared using both the PD and SID similarity parameters. The results revealed that the average source profiles presented low PD but high SID, with overall values outside the acceptance box (PD < 0.4 and SID < 0.8), indicating that they were different over the different source profiles of this study. For all profiles, the variability in the PD–SID space did not reach the similarity acceptance box, which suggests that all organic source profiles may be different from most organic compounds emitted from multiple types of sources, as is expected when the molecular organic markers approach is used to distinguish between source profiles [14]. It is important to note that enrichment in some organic compounds contributes to the distinction among source profiles of the same category. A similar behavior was observed from the COD analysis. The COD range values ranged from 0.63 to 0.72, suggesting a slight dissimilarity among source profiles (values tend to be closer to 1 than to 0) [58].

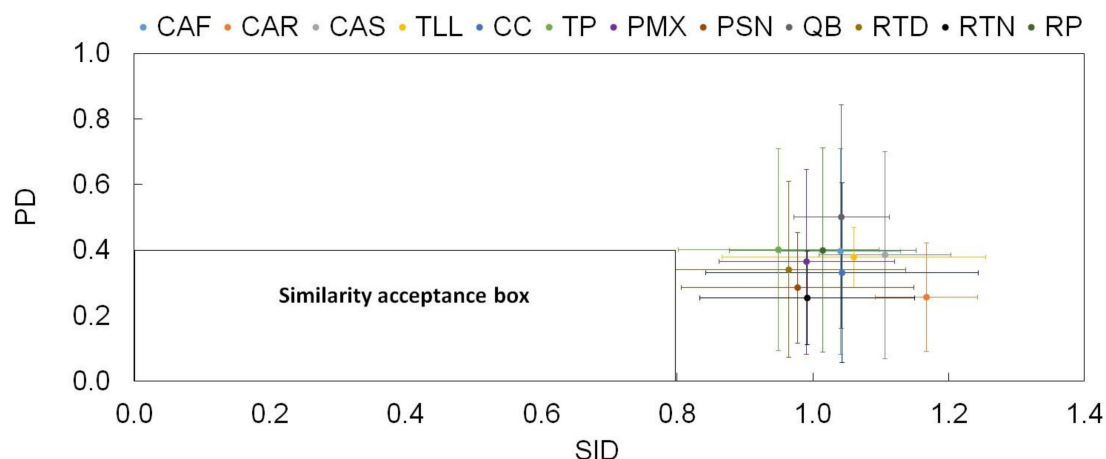


Figure 10. Similarity test among the source emission profiles based on the PD and the SID as per Belis and Pernigotti [59]. The bars represent the range values for each parameter among source profiles. Definition of source profile codes are presented in Table 1.

For individual organic compound quantification, an uncertainty of $\pm 20\%$ of the measured concentration was used for all source profiles [13,24,107–109]. In addition, an error propagation technique was followed to estimate the final uncertainties [109]. The estimated final uncertainties for each source profile can be observed in Table S2 of the Supplementary Material.

4. Conclusions

The organic composition of $PM_{2.5}$ samples collected from 12 anthropogenic sources in the MMA were obtained, quantifying 72 organic compounds. Following a ground-based source-dominated approach along with molecular organic marker approach assures the representativeness with a low number of samples. The organic source profiles of these sources were quite distinguishable, as determined by PD and SID and CODs for each pair of organic source profiles. It can be observed that diesel and gasoline vehicle traffic profiles were dominated by LMW-PAHs and HMW-PAHs which are considered carcinogenic and mutagenic organic compounds. There was a difference between industrial parks and the oil refinery: the first ones are dominated by *n*-alkanes indicating the use of fossil fuels in their processes while the second one is dominated by hopanes. Meat charbroiling operation profiles were dominated by cholesterol and levoglucosan while other cooking activities, not involving charcoal, saw very low levels of levoglucosan, highlighting the importance of fuel in cooking emissions. The urban background profiles in this study are a combination of secondary organic markers, *n*-alkanoic acids and hopanes. The biomass burning profiles are dominated by methoxyphenols and resin acids; all fires derived from trash or forest burning represent a potential source of the organic compounds. The relevance of these profiles resides on their potential application to conduct further source apportionment studies in Mexico, a region for which, to date, no local source profiles exist. These profiles can be used as receptor model input or for model output validation. This source profile data finds application also to validate emissions inventories derived from bottom-up approaches. Results from these applications can be used to outline strategies to reduce fine PM air pollution from specific emission sources as well as to quantify health impacts from specific air toxics.

Supplementary Materials: The following are available online at <https://www.mdpi.com/article/10.3390/atmos12050554/s1>, Table S1: organic composition of organic markers (ng/mg) for each source emission profile. Table S2: organic composition uncertainty of organic markers (ng/mg) for each source emission profile.

Author Contributions: Conceptualization, A.M.; methodology, Y.M., P.H., M.P.F. and A.M.; validation, Y.M. and P.H.; formal analysis, Y.M., G.M. and L.T.G.; investigation, Y.M. and G.M.; resources, P.H., M.P.F. and A.M.; data curation, Y.M. and G.M.; writing—original draft preparation, Y.M. and G.M.; writing—review and editing, Y.M., L.T.G., P.H., M.P.F. and A.M.; supervision, Y.M., P.H. and A.M.; project administration, A.M.; funding acquisition, A.M. All authors have read and agreed to the published version of the manuscript.

Funding: This research was funded by the Mexican National Council for Science and Technology (CONACYT), grant number CB-2010-154122. G. Medina received additional support (scholarship, grant number 293926) through CONACYT during his research stay at Tecnológico de Monterrey.

Institutional Review Board Statement: Not applicable.

Informed Consent Statement: Not applicable.

Data Availability Statement: The data presented in this study are available in the article's accompanying Supplementary Materials.

Conflicts of Interest: The authors declare no conflict of interest.

References

1. Jacobson, M.C.; Hansson, H.-C.; Noone, K.J.; Charlson, R.J. Organic atmospheric aerosols: Review and state of the science. *Rev. Geophys.* **2000**, *38*, 267–294. [[CrossRef](#)]
2. Grahame, T.J.; Klemm, R.; Schlesinger, R.B. Public health and components of particulate matter: The changing assessment of black carbon. *J. Air Waste Manag. Assoc.* **2014**, *64*, 620–660. [[CrossRef](#)]
3. Atkinson, R.W.; Mills, I.C.; Walton, H.A.; Anderson, H.R. Fine particle components and health—A systematic review and meta-analysis of epidemiological time series studies of daily mortality and hospital admissions. *J. Expo. Sci. Environ. Epidemiol.* **2015**, *25*, 208–214. [[CrossRef](#)] [[PubMed](#)]
4. Srivastava, D.; Favez, O.; Perraudin, E.; Villenave, E.; Albinet, A. Comparison of Measurement-Based Methodologies to Apportion Secondary Organic Carbon (SOC) in PM_{2.5}: A Review of Recent Studies. *Atmosphere* **2018**, *9*, 452. [[CrossRef](#)]
5. Christiansen, A.E.; Carlton, A.G.; Porter, W.C. Changing Nature of Organic Carbon over the United States. *Environ. Sci. Technol.* **2020**, *54*, 10524–10532. [[CrossRef](#)] [[PubMed](#)]
6. McNeill, V.F. Atmospheric Aerosols: Clouds, Chemistry, and Climate. *Annu. Rev. Chem. Biomol. Eng.* **2017**, *8*, 427–444. [[CrossRef](#)]
7. Mukherjee, A.; Agrawal, M. World air particulate matter: Sources, distribution and health effects. *Environ. Chem. Lett.* **2017**, *15*, 283–309. [[CrossRef](#)]
8. Noziere, B.; Kalberer, M.; Claeys, M.; Allan, J.; D'Anna, B.; Decesari, S.; Finessi, E.; Glasius, M.; Grgic, I.; Hamilton, J.F.; et al. The molecular identification of organic compounds in the atmosphere: State of the art and challenges. *Chem. Rev.* **2015**, *115*, 3919–3983. [[CrossRef](#)]
9. Pirhadi, M.; Mousavi, A.; Taghvaei, S.; Shafer, M.M.; Sioutas, C. Semi-volatile components of PM_{2.5} in an urban environment: Volatility profiles and associated oxidative potential. *Atmos. Environ.* **2020**, *223*, 117197. [[CrossRef](#)]
10. Klyta, J.; Czaplicka, M. Determination of secondary organic aerosol in particulate matter—Short review. *Microchem. J.* **2020**, *157*, 104997. [[CrossRef](#)]
11. Ali, M.U.; Liu, G.; Yousaf, B.; Ullah, H.; Abbas, Q.; Munir, M.A.M. A systematic review on global pollution status of particulate matter-associated potential toxic elements and health perspectives in urban environment. *Environ. Geochem. Health* **2019**, *41*, 1131–1162. [[CrossRef](#)]
12. Schauer, J.J.; Rogge, W.F.; Hildemann, L.M.; Mazurek, M.A.; Cass, G.R.; Simoneit, B.R.T. Source apportionment of airborne particulate matter using organic compounds as tracers. *Atmos. Environ.* **1996**, *30*, 3837–3855. [[CrossRef](#)]
13. Schauer, J.J.; Cass, G.R. Source apportionment and particle phase air pollutants using organic compounds as tracers. *Environ. Sci. Technol.* **2000**, *34*, 1821–1832. [[CrossRef](#)]
14. Lin, L.; Lee, M.L.; Eatough, D.J. Review of recent advances in detection of organic markers in fine particulate matter and their use for source apportionment. *J. Air Waste Manag. Assoc.* **2010**, *60*, 3–25. [[CrossRef](#)]
15. Calvo, A.; Alves, C.; Castro, A.; Pont, V.; Vicente, A.; Fraile, R. Research on Aerosol Sources and Chemical Composition: Past, Current and Emerging Issues. *Atmos. Res.* **2013**, *120*, 1–28. [[CrossRef](#)]
16. Belis, C.A.; Karagulian, F.; Larsen, B.R.; Hopke, P.K. Critical review and meta-analysis of ambient particulate matter source apportionment using receptor models in Europe. *Atmos. Environ.* **2013**, *69*, 94–108. [[CrossRef](#)]
17. Hopke, P.K.; Dai, Q.; Li, L.; Feng, Y. Global review of recent source apportionments for airborne particulate matter. *Sci. Total Environ.* **2020**, *740*, 140091. [[CrossRef](#)]
18. Hopke, P.K. Review of receptor modeling methods for source apportionment. *J. Air Waste Manag. Assoc.* **2016**, *66*, 237–259. [[CrossRef](#)]
19. Cai, T.; Schauer, J.J.; Huang, W.; Fang, D.; Shang, J.; Wang, Y.; Zhang, Y. Sensitivity of source apportionment results to mobile source profiles. *Environ. Pollut.* **2016**, *219*, 821–828. [[CrossRef](#)]

20. Mancilla, Y.; Herckes, P.; Fraser, M.P.; Mendoza, A. Secondary organic aerosol contributions to PM_{2.5} in Monterrey, Mexico: Temporal and seasonal variation. *Atmos. Res.* **2015**, *153*, 348–359. [CrossRef]
21. Martínez-Cinco, M.; Santos-Guzmán, J.; Mejía-Velázquez, G. Source apportionment of PM_{2.5} for supporting control strategies in the Monterrey Metropolitan Area, Mexico. *J. Air Waste Manag. Assoc.* **2016**, *66*, 631–642. [CrossRef] [PubMed]
22. González-Santiago, O. Determinación del Contenido de PAH's en Partículas PM_{2.5} en una Zona de alto tráfico Vehicular y Otra con Potencial Exposición Industrial del Área Metropolitana de Monterrey. Ph.D. Thesis, Facultad de Ciencias Químicas, Universidad Autónoma de Nuevo León (UANL), San Nicolás de los Garza, NL, Mexico, 2009. Available online: <http://eprints.uanl.mx/1959/1/1080186668.pdf> (accessed on 5 March 2021).
23. López-Ayala, O.; González-Hernández, L.T.; Alcantar-Rosales, V.M.; Elizarragaz de la Rosa, D.; Heras-Ramírez, M.E.; Silva-Vidaurri, L.G.; Alfaro-Barbosa, J.M.; Gaspar-Ramírez, O. Levels of polycyclic aromatic hydrocarbons associated with particulate matter in a highly urbanized and industrialized region in northeastern Mexico. *Atmos. Pollut. Res.* **2019**, *10*, 1655–1662. [CrossRef]
24. Mancilla, Y.; Mendoza, A.; Fraser, M.P.; Herckes, P. Organic composition and source apportionment of fine aerosol at Monterrey, Mexico, based on organic markers. *Atmos. Chem. Phys.* **2016**, *16*, 953–970. [CrossRef]
25. Stone, E.; Snyder, D.; Sheelsey, R.; Sullivan, A.; Weber, R.; Schauer, J. Source Apportionment of Fine Organic Aerosol in Mexico City During the MILAGRO Experiment 2006. *Atmos. Chem. Phys.* **2008**, *8*, 1249–1259. [CrossRef]
26. Martínez-Cinco, M.A.; Caballero, P.; Carrillo, O.; Mendoza, A.; Mejía, M.G. Chemical characterization and factor analysis of PM_{2.5} in two sites of Monterrey, Mexico. *J. Air Waste Manag. Assoc.* **2012**, *62*, 817–827. [CrossRef]
27. Secretaría de Desarrollo Sustentable; Secretaría de Medio Ambiente y Recursos Naturales. *Programa de Gestión para Mejorar la Calidad del Aire del Estado de Nuevo León ProAire 2016–2025*; Gobierno de Estado de Nuevo León: Monterrey, Mexico, 2016. Available online: https://www.gob.mx/cms/uploads/attachment/file/250974/ProAire_Nuevo_Leon.pdf (accessed on 20 June 2020).
28. Chow, J.C.; Watson, J.G.; Kuhns, H.; Etyemezian, V.; Lowenthal, D.H.; Crow, D.; Kohl, S.D.; Engelbrecht, J.P.; Green, M.C. Source profiles for industrial, mobile, and area sources in the Big Bend Regional Aerosol Visibility and observational study. *Chemosphere* **2004**, *54*, 185–208. [CrossRef]
29. Pulong, C.; Tijian, W.; Mei, D.; Kasoar, M.; Yong, H.; Min, X.; Shu, L.; Bingliang, Z.; Mengmeng, L.; Tunan, H. Characterization of major natural and anthropogenic source profiles for size-fractionated PM in Yangtze River Delta. *Sci. Total Environ.* **2017**, *598*, 135–145. [CrossRef]
30. Mancilla, Y.; Mendoza, D. A tunnel study to characterize PM_{2.5} emissions from gasoline-powered vehicles in Monterrey, Mexico. *Atmos. Environ.* **2012**, *59*, 449–460. [CrossRef]
31. Plewka, A.; Gnauk, T.; Brüggemann, E.; Neusüss, C.; Herrmann, H. Size-resolved aerosol characterization for a polluted episode at the IfT research station Melpitz in autumn 1997. *J. Atmos. Chem.* **2004**, *48*, 131–156. [CrossRef]
32. Birch, M.E.; Cary, R.A. Elemental Carbon-Based Method for Monitoring Occupational Exposures to Particulate Diesel Exhaust. *Aerosol Sci. Tech.* **1996**, *25*, 221–241. [CrossRef]
33. Brown, S.; Herckes, P.; Ashbaugh, L.; Hannigan, M.; Kreidenweis, S.; Collett, J. Characterization of Organic Aerosol in Big Bend National Park, Texas. *Atmos. Environ.* **2002**, *26*, 5807–5818. [CrossRef]
34. Tsapakis, M.; Lagoudaki, E.; Stephanou, E.G.; Kavouras, I.G.; Koutrakis, P.; Oyola, P.; von Baer, D. The composition and sources of PM_{2.5} organic aerosol in two urban areas of Chile. *Atmos. Environ.* **2002**, *36*, 3851–3863. [CrossRef]
35. Harrad, S.; Hassoun, S.; Callén Romero, M.S.; Harrison, R.M. Characterisation and source attribution of the semi-volatile organic content of atmospheric particles and associated vapour phase in Birmingham, UK. *Atmos. Environ.* **2003**, *37*, 4985–4991. [CrossRef]
36. Kalaitzoglou, M.; Terzi, E.; Samara, C. Patterns and sources of particle-phase aliphatic and polycyclic aromatic hydrocarbons in urban and rural sites of western Greece. *Atmos. Environ.* **2004**, *38*, 2545–2560. [CrossRef]
37. Feng, J.; Hu, M.; Chan, C.K.; Lau, P.S.; Fang, M.; He, L.; Tang, X. A comparative study of the organic matter in PM_{2.5} from three Chinese megacities in three different climatic zones. *Atmos. Environ.* **2006**, *40*, 3983–3994. [CrossRef]
38. Kang, M.; Ren, L.; Ren, H.; Zhao, Y.; Kawamura, K.; Zhang, H.; Wei, L.; Sun, Y.; Wang, Z.; Fu, P. Primary biogenic and anthropogenic sources of organic aerosols in Beijing, China: Insights from saccharides and n-alkanes. *Environ. Pollut.* **2018**, *243*, 1579–1587. [CrossRef]
39. Li, J.; Wang, G.; Aggarwal, S.G.; Huang, Y.; Ren, Y.; Zhou, B.; Singh, K.; Gupta, P.K.; Cao, J.; Zhang, R. Comparison of abundances, compositions and sources of elements, inorganic ions and organic compounds in atmospheric aerosols from Xi'an and New Delhi, two megacities in China and India. *Sci. Total Environ.* **2014**, *485*–495. [CrossRef]
40. Esmailirad, S.; Lai, A.; Abbaszade, G.; Schnelle-Kreis, J.; Zimmermann, R.; Uzu, G.; Daellenbach, K.; Canonaco, F.; Hassankhany, H.; Arhami, M.; et al. Source apportionment of fine particulate matter in a middle eastern metropolis, Tehran-Iran, using PMF with organic and inorganic markers. *Sci. Total Environ.* **2020**, *705*, 135330. [CrossRef]
41. Gelencsér, A. *Carbonaceous Aerosol: Atmospheric and Oceanographic Sciences Library*; Springer Publications: Dordrecht, The Netherlands, 2004; pp. 184–190.
42. Kang, M.; Fu, P.; Aggarwal, S.G.; Kumar, S.; Zhao, Y.; Sun, Y.; Wang, Z. Size distributions of n-alkanes, fatty acids and fatty alcohols in springtime aerosols from New Delhi, India. *Environ. Pollut.* **2016**, *219*, 957–966. [CrossRef]
43. Pateraki, S.; Manousakas, M.; Bairachtari, K.; Kantarelou, V.; Eleftheriadis, K.; Vasilakos, C.; Assimakopoulos, V.D.; Maggos, T. The traffic signature on the vertical PM profile: Environmental and health risks within an urban roadside environment. *Sci. Total Environ.* **2019**, *646*, 448–459. [CrossRef]

44. Romagnoli, P.; Balducci, C.; Perilli, M.; Esposito, G.; Cecinato, A. Organic molecular markers in marine aerosols over the western mediterranean sea. *Environ. Pollut.* **2019**, *248*, 145–458. [[CrossRef](#)] [[PubMed](#)]
45. Young, L.-H.; Wang, C.-S. Characterization of *n*-alkanes in PM_{2.5} of the Taipei aerosol. *Atmos. Environ.* **2002**, *36*, 477–482. [[CrossRef](#)]
46. Sklorz, M.; Schnelle-Kreis, J.; Liu, Y.; Orasche, J.; Zimmermann, R. Daytime resolved analysis of polycyclic aromatic hydrocarbons in urban aerosol samples—Impact of sources and meteorological conditions. *Chemosphere* **2007**, *67*, 934–943. [[CrossRef](#)] [[PubMed](#)]
47. Dvorská, A.; Lammel, G.; Klánová, J. Use of diagnostic ratios for studying source apportionment and reactivity of ambient polycyclic aromatic hydrocarbons over central Europe. *Atmos. Environ.* **2011**, *45*, 420–427. [[CrossRef](#)]
48. Katsoyiannis, A.; Sweetman, A.J.; Jones, K.C. PAH molecular diagnostic ratios applied to atmospheric sources: A critical evaluation using two decades of source inventory and air concentration data from UK. *Environ. Sci. Technol.* **2011**, *45*, 8897–8906. [[CrossRef](#)]
49. Chen, F.; Hu, W.; Zhong, Q. Emissions of particle-phase polycyclic aromatic hydrocarbons (PAHs) in the Fu Gui-shan Tunnel of Nanjing, China. *Atmos. Res.* **2013**, *124*, 53–60. [[CrossRef](#)]
50. Alves, C.A.; Vicente, A.M.P.; Gomes, J.; Nunes, T.; Duarte, M.; Bandowe, B.A.M. Polycyclic aromatic hydrocarbons (PAHs) and their derivatives (oxygenated-PAHs, nitrated-PAHs and azaarenes) in size-fractionated particles emitted in an urban road tunnel. *Atmos. Res.* **2016**, *180*, 128–137. [[CrossRef](#)]
51. Demir, T.; Yenisoý-Karakaş, S.; Karakaş, D. PAHs, elemental and organic carbons in a highway tunnel atmosphere and road dust: Discrimination of diesel and gasoline emissions. *Build. Environ.* **2019**, *160*, 106166. [[CrossRef](#)]
52. Mao, Y.; Hu, T.; Shi, M.; Cheng, C.; Liu, W.; Zhang, J.; Qi, S.; Xing, X. PM_{2.5}-bound PAHs during a winter haze episode in a typical mining city, central China: Characteristics, influencing parameters, and sources. *Atmos. Pollut. Res.* **2020**, *11*, 131–140. [[CrossRef](#)]
53. Tobiszewski, M.; Namieśnik, J. PAH diagnostic ratios for the identification of pollution emission sources. *Environ. Pollut.* **2012**, *162*, 110–119. [[CrossRef](#)]
54. Kong, S.; Ji, Y.; Li, Z.; Lu, B.; Bai, Z. Emission and profile characteristic of polycyclic aromatic hydrocarbons in PM_{2.5} and PM₁₀ from stationary sources based on dilution sampling. *Atmos. Environ.* **2013**, *77*, 155–165. [[CrossRef](#)]
55. Liu, Y.; Gao, Y.; Yu, N.; Zhang, C.; Wang, S.; Ma, L.; Zhao, J.; Lohmann, R. Particulate matter, gaseous and particulate polycyclic aromatic hydrocarbons (PAHs) in an urban traffic tunnel of China: Emission from on-road vehicles and gas-particle partitioning. *Chemosphere* **2015**, *134*, 52–59. [[CrossRef](#)]
56. Zhu, Y.; Yang, L.; Meng, C.; Yuan, Q.; Yan, C.; Dong, C.; Sui, X.; Yao, L.; Yang, F.; Lu, Y.; et al. Indoor/outdoor relationships and diurnal/nocturnal variations in water-soluble ion and PAH concentrations in the atmospheric PM_{2.5} of a business office area in Jinan, a heavily polluted city in China. *Atmos. Res.* **2015**, *153*, 276–285. [[CrossRef](#)]
57. Zhang, F.; Zhang, R.; Guan, M.; Shu, Y.; Shen, L.; Chen, X.; Li, T. Polycyclic aromatic hydrocarbons (PAHs) and Pb isotopic ratios in a sediment core from Shilianghe Reservoir, eastern China: Implying pollution sources. *Appl. Geochem.* **2016**, *66*, 140–148. [[CrossRef](#)]
58. Zhang, N.; Han, B.; He, F.; Xu, J.; Zhao, R.; Zhang, Y.; Bai, Z. Chemical characteristic of PM_{2.5} emission and inhalational carcinogenic risk of domestic Chinese cooking. *Environ. Pollut.* **2017**, *227*, 24–30. [[CrossRef](#)]
59. Belis, C.A.; Pernigotti, D. DeltaSA tool for source apportionment benchmarking, description and sensitivity analysis. *Atmos. Environ.* **2018**, *180*, 138–148. [[CrossRef](#)]
60. Weber, S.; Salameh, D.; Albinet, A.; Alleman, L.Y.; Waked, A.; Besombes, J.-L.; Jacob, V.; Guillaud, G.; Meshbah, B.; Rocq, B.; et al. Comparison of PM₁₀ Sources Profiles at 15 French Sites Using a Harmonized Constrained Positive Matrix Factorization Approach. *Atmosphere* **2019**, *10*, 310. [[CrossRef](#)]
61. Karagulian, F.; Belis, C.A.; Dora, C.F.; Prüss-Ustün, A.M.; Bonjour, S.; Adair-Rohani, H.; Amann, M. Contributions to cities' ambient particulate matter (PM): A systematic review of local source contributions at global level. *Atmos. Environ.* **2015**, *120*, 475–483. [[CrossRef](#)]
62. Pinto, J.P.; Lefohn, A.S.; Shadwick, D.S. Spatial variability of PM_{2.5} in urban areas in the United States. *J. Air Waste Manag. Assoc.* **2004**, *54*, 440–449. [[CrossRef](#)]
63. Simoneit, B.R.T.; Kobayashi, M.; Mochida, M.; Kawamura, K.; Lee, M.; Lim, H.-J.; Turpin, B.; Komazaki, Y. Composition and major sources of organic compounds of aerosol particulate matter sampled during the ACE-Asia campaign. *J. Geophys. Res. Atmos.* **2004**, *109*, 1–22. [[CrossRef](#)]
64. Rogge, W.F.; Hildemann, L.M.; Mazurek, M.A.; Cass, G.R.; Simoneit, B.R.T. Sources of fine organic aerosol. 2. Noncatalyst and catalyst-equipped automobiles and Heavy-duty diesel trucks. *Environ. Sci. Technol.* **1993**, *27*, 636–651. [[CrossRef](#)]
65. Phuleria, H.C.; Sheesley, R.J.; Schauer, J.J.; Fine, P.M.; Sioutas, C. Roadside measurements of size-segregated particulate organic compounds near gasoline and diesel-dominated freeways in Los Angeles, CA. *Atmos. Environ.* **2007**, *41*, 4653–4671. [[CrossRef](#)]
66. Pérez Pastor, R.; Salvador, P.; García Alonso, S.; Alastuey, A.; García dos Santos, S.; Querol, X.; Artiñano, B. Characterization of organic aerosol at a rural site influenced by olive waste biomass burning. *Chemosphere* **2020**, *248*, 125896. [[CrossRef](#)]
67. Simoneit, B.R.T.; Mazurek, M.A. Organic matter of the troposphere—II. Natural background of biogenic lipid matter in aerosols over the rural western United States. *Atmos. Environ.* **1982**, *16*, 2139–2159. [[CrossRef](#)]
68. Seigler, D.S. Plant Waxes. In *Plant Secondary Metabolism*; Springer: Boston, MA, USA, 1998. [[CrossRef](#)]
69. Cai, T.; Zhang, Y.; Fang, D.; Shang, J.; Zhang, Y.; Zhang, Y. Chinese vehicle emissions characteristic testing with small sample size: Results and comparison. *Atmos. Pollut. Res.* **2017**, *8*, 154–163. [[CrossRef](#)]

70. Schauer, J.J.; Kleeman, M.J.; Cass, G.R.; Simoneit, B.R.T. Measurement of Emissions from Air Pollution Sources. 3. C1-C29 Organic Compounds from Fireplace Combustion of Wood. *Environ. Sci. Technol.* **2001**, *35*, 1716–1728. [[CrossRef](#)] [[PubMed](#)]
71. Kawamura, K.; Ishimura, Y.; Yamazaki, K. Four years' observations of terrestrial lipid class compounds in marine aerosols from the western North Pacific. *Glob. Biogeochem. Cycles* **2003**, *17*, 1–3. [[CrossRef](#)]
72. Yadav, S.; Tandon, A.; Attri, A.K. Monthly and seasonal variations in aerosol associated n-alkane profiles in relation to meteorological parameters in New Delhi, India. *Aerosol Air Qual. Res.* **2013**, *13*, 287–300. [[CrossRef](#)]
73. Shrivastava, M.K.; Subramanian, R.; Rogge, W.F.; Robinson, A.L. Sources of organic aerosol: Positive matrix factorization of molecular marker data and comparison of results from different source apportionment models. *Atmos. Environ.* **2007**, *41*, 9353–9369. [[CrossRef](#)]
74. Simoneit, B.R.T. Biomass burning—a review of organic tracers for smoke from incomplete combustion. *Appl. Geochem.* **2002**, *17*, 129–162. [[CrossRef](#)]
75. Vila-Escalé, M.; Vegas-Vilarrúbia, T.; Prat, N. Release of polycyclic aromatic compounds into a Mediterranean creek (Catalonia, NE Spain) after a forest fire. *Water Resour.* **2007**, *41*, 2171–2179. [[CrossRef](#)] [[PubMed](#)]
76. Marr, L.C.; Grogan, L.A.; Wöhrschimmel, H.; Molina, L.T.; Molina, M.J.; Smith, T.J.; Garshick, E. Vehicle traffic as a source of particulate polycyclic aromatic hydrocarbon exposure in the Mexico City metropolitan area. *Environ. Sci. Technol.* **2004**, *38*, 2584–2592. [[CrossRef](#)] [[PubMed](#)]
77. Wang, C.; Meng, Z.; Yao, P.; Zhang, L.; Wang, Z.; Lv, Y.; Tian, Y.; Feng, Y. Sources-specific carcinogenicity and mutagenicity of PM_{2.5}-bound PAHs in Beijing, China: Variations of contributions under diverse anthropogenic activities. *Ecotox. Environ. Safe.* **2019**, *183*, 109552. [[CrossRef](#)] [[PubMed](#)]
78. Ramdahl, T. Retene—A molecular marker of wood combustion in ambient air. *Nature* **1983**, *306*, 580–582. [[CrossRef](#)]
79. Schauer, J.J.; Kleeman, M.J.; Cass, G.R.; Simoneit, B.R.T. Measurement of Emissions from Air Pollution Sources. 4. C1-C27 Organic Compounds from Cooking with Seed Oils. *Environ. Sci. Technol.* **2002**, *36*, 567–575. [[CrossRef](#)]
80. Schauer, J.J.; Kleeman, M.J.; Cass, G.R.; Simoneit, B.R.T. Measurement of emissions from Air Pollution Sources. 5. C1-C32 Organic Compounds from Gasoline-Powered Motor Vehicles. *Environ. Sci. Technol.* **2002**, *36*, 1169–1180. [[CrossRef](#)]
81. Schauer, J.J.; Kleeman, M.J.; Cass, G.R.; Simoneit, B.R.T. Measurements of emissions from air pollution sources. 2. C1 through C30 organic compounds from medium duty diesel trucks. *Environ. Sci. Technol.* **1999**, *33*, 1578–1587. [[CrossRef](#)]
82. Rogge, W.F.; Hildemann, L.M.; Mazurek, M.A.; Cass, G.R.; Simoneit, B.R.T. Sources of fine organic aerosol. 5. Natural gas home appliances. *Environ. Sci. Technol.* **1993**, *27*, 2736–2744. [[CrossRef](#)]
83. Zhao, X.; Wang, X.; Ding, X.; He, Q.; Zhang, Z.; Liu, T.; Fu, X.; Gao, B.; Wang, Y.; Zhang, Y.; et al. Composition and sources of organic acids in fine particles (PM_{2.5}) over the Pearl River Delta region, south China. *J. Environ. Sci.* **2014**, *26*, 110–121. [[CrossRef](#)]
84. Zhao, X.; Hu, Q.; Wang, X.; Ding, X.; He, Q.; Zhang, Z.; Shen, R.; Lü, S.; Liu, T.; Fu, X. Composition profiles of organic aerosols from Chinese residential cooking: Case study in urban Guangzhou, south China. *J. Atmos. Chem.* **2015**, *72*, 1–18. [[CrossRef](#)]
85. Schauer, J.J.; Kleeman, M.J.; Cass, G.R.; Simoneit, B.R.T. Measurement of Emissions from Air Pollution Sources. 1. C1 through C29 organic compounds from meat charbroiling. *Environ. Sci. Technol.* **1999**, *33*, 1566–1577. [[CrossRef](#)]
86. Robinson, A.L.; Subramanian, R.; Donahue, N.M.; Bernardo-Bricker, A.; Rogge, W.F. Source apportionment of molecular markers and organic aerosol. 2. Biomass smoke. *Environ. Sci. Technol.* **2006**, *40*, 7811–7819. [[CrossRef](#)]
87. Alves, C.A.; Vicente, A.; Monteiro, C.; Gonçalves, C.; Evtugina, M.; Pio, C. Emission of trace gases and organic components in smoke particles from wildfire in a mixed-evergreen forest in Portugal. *Sci. Total Environ.* **2011**, *409*, 1466–1475. [[CrossRef](#)]
88. Gonçalves, C.; Alves, C.; Fernandes, A.P.; Monteiro, C.; Tarelho, L.; Evtugina, M.; Pio, C. Organic compounds in PM_{2.5} emitted from fireplace and woodstove combustion of typical Portuguese wood species. *Atmos. Environ.* **2011**, *45*, 4533–4545. [[CrossRef](#)]
89. Latif, M.T.; Anuwar, N.Y.; Srithawirat, T.; Razak, I.S.; Ramli, N.A. Composition of levoglucosan and surfactants in atmospheric aerosols from biomass burning. *Aerosol Air Qual. Res.* **2011**, *11*, 837–845. [[CrossRef](#)]
90. Vicente, E.D.; Alves, C.A. An overview of particulate emissions from residential biomass combustion. *Atmos. Res.* **2018**, *199*, 159–185. [[CrossRef](#)]
91. Rogge, W.F.; Hildemann, L.M.; Mazurek, M.A.; Cass, G.R.; Simoneit, B.R.T. Sources of fine organic aerosol. 1. Charbroilers and meat cooking operations. *Environ. Sci. Technol.* **1991**, *25*, 1112–1125. [[CrossRef](#)]
92. Robinson, A.L.; Subramanian, R.; Donahue, N.M.; Bernardo-Bricker, A.; Rogge, W.F. Source apportionment of molecular markers and organic aerosol. 3. Food cooking emissions. *Environ. Sci. Technol.* **2006**, *40*, 7820–7827. [[CrossRef](#)]
93. Wang, Q.; Shao, M.; Zhang, Y.; Wei, Y.; Hu, M.; Guo, S. Source apportionment of fine organic aerosol in Beijing. *Atmos. Chem. Phys.* **2009**, *9*, 8573–8585. [[CrossRef](#)]
94. Wu, X.; Cao, F.; Haque, M.; Fan, M.-Y.; Zhang, S.-C.; Zhang, Y.-L. Molecular composition and source apportionment of fine organic aerosols in Northeast China. *Atmos. Environ.* **2020**, 117722. [[CrossRef](#)]
95. Eatough, D.J.; Benner, C.L.; Tang, H.; Landon, V.; Richards, G.; Caka, F.M.; Crawford, J.; Lewis, E.A.; Hansen, L.D.; Eatough, N.L. The chemical composition of environmental tobacco smoke III. Identification of conservative tracers of environmental tobacco smoke. *Environ. Int.* **1989**, *15*, 19–28. [[CrossRef](#)]
96. Rogge, W.F.; Hildemann, L.M.; Mazurek, M.A.; Cass, G.R.; Simoneit, B.R.T. Sources of fine organic aerosol. 6. Cigarette smoke in the urban atmosphere. *Environ. Sci. Technol.* **1994**, *28*, 1375–1388. [[CrossRef](#)]
97. Hildemann, L.M.; Markowski, G.R.; Cass, G.R. Chemical composition of emissions from urban sources of fine organic aerosol. *Environ. Sci. Technol.* **1991**, *25*, 744–759. [[CrossRef](#)]

98. Gaston, C.J.; Lopez-Hilfiker, F.D.; Whybrew, L.E.; Hadley, O.; McNair, F.; Gao, H.; Jaffe, D.A.; Thornton, J.A. Online molecular characterization of fine particulate matter in Port Angeles, WA: Evidence for a major impact from residential wood smoke. *Atmos. Environ.* **2016**, *138*, 99–107. [[CrossRef](#)]
99. Linuma, Y.; Keywood, M.; Herrmann, H. Characterization of primary and secondary organic aerosol in Melbourne airshed: The influence of biogenic emissions, wood smoke and bushfires. *Atmos. Environ.* **2016**, *130*, 54–63. [[CrossRef](#)]
100. Bergauff, M.; Ward, T.; Noonan, C.; Palmer, C.P. Determination and evaluation of selected organic chemical tracers for wood smoke in airborne particulate matter. *Int. J. Environ. An. Ch.* **2008**, *88*, 473–486. [[CrossRef](#)]
101. Simpson, C.D.; Paulsen, M.; Dills, R.L.; Liu, L.J.S.; Kalman, D.A. Determination of methoxyphenols in ambient atmospheric particulate matter: Tracers for wood combustion. *Environ. Sci. Tech.* **2005**, *39*, 631–637. [[CrossRef](#)]
102. Oros, D.R.; Simoneit, B.R.T. Identification and emission factors of molecular tracers in organic aerosols from biomass burning: Part 2. Deciduous trees. *Appl. Geochem.* **2001**, *16*, 1545–1565. [[CrossRef](#)]
103. Jia, L.; Xu, Y. The role of functional groups in the understanding of secondary organic aerosol formation mechanism from α -pinene. *Sci. Total. Environ.* **2020**, *738*, 139831. [[CrossRef](#)]
104. Christoffersen, T.S.; Hjorth, J.; Horie, O.; Jensen, N.R.; Kotzias, D.; Molander, L.L.; Neeb, P.; Rupper, L.; Winterhalter, R.; Virkkula, A.; et al. cis-pinonic acid, a possible precursor for organic aerosol formation from ozonolysis of α -pinene. *Atmos. Environ.* **1998**, *32*, 1657–1661. [[CrossRef](#)]
105. Bhat, S.; Fraser, M.P. Primary source attribution and analysis of α -pinene photooxidation products in Duke Forest, North Carolina. *Atmos. Environ.* **2007**, *41*, 2958–2966. [[CrossRef](#)]
106. Ding, X.; Wang, X.M.; Zheng, M. The influence of temperature and aerosol acidity on biogenic secondary organic aerosol tracers: Observations at a rural site in the central Pearl River Delta region, South China. *Atmos. Environ.* **2011**, *45*, 1303–1311. [[CrossRef](#)]
107. Fraser, M.P.; Yue, Z.W.; Buzcu, B. Source apportionment of fine particulate matter in Houston, TX, using organic molecular markers. *Atmos. Environ.* **2003**, *37*, 2117–2123. [[CrossRef](#)]
108. Nakashima, S.; Hayashi, Y. Determination of detection limits and quantification limits for compounds in a database of GC/MS by FUMI theory. *Mass Spectrom.* **2016**, *5*, 1–6. [[CrossRef](#)]
109. Taylor, J.R. Propagation of uncertainties. In *An Introduction to Error Analysis: The Study of Uncertainties in Physical Measurement*, 2nd ed.; University Science Books: Mill Valley, CA, USA, 1997; pp. 45–79.